Technische Universiteit Delft
Faculteit Elektrotechniek, Wiskunde en Informatica
Delft Institute of Applied Mathematics

Bepaling van het mechanisme achter de vorming van spatio-temporele hexagonale activiteitspatronen in een neuronaal netwerk model

(Engelse titel: Determination of the mechanism behind the formation of spatio-temporal hexagonal activity patterns in a model neuronal network)

Verslag ten behoeve van het
Delft Institute for Applied Mathematics
als onderdeel ter verkrijging

van de graad van

BACHELOR OF SCIENCE
in
TECHNISCHE WISKUNDE

door

D.C. Koppenol, M.Sc.

Delft, Nederland
Februari 2012

BSc verslag TECHNISCHE WISKUNDE

"Bepaling van het mechanisme achter de vorming van spatio-temporele hexagonale activiteitspatronen in een neuronaal netwerk model"

(Engelse titel: "Determination of the mechanism behind the formation of spatio-temporal hexagonal activity patterns in a model neuronal network)"

D.C. Koppenol, M.Sc.

Technische Universiteit Delft

Begeleider

Dr. J.L.A. Dubbeldam

Overige commissieleden

Dr.ing. D. Jeltsema, M.Sc.	Dr. J.G. Spandaw
. . .	. . .
Februari, 2012	Delft

To my wife Gabriela, for her love, peace and understanding

Acknowledgments

I would like to thank Johan Dubbeldam for his support, advice and insightful comments throughout the supervision of this project. Furthermore I would like to thank him for giving me independence in pursuing research; I've learned a lot about various mathematical techniques which can be applied in mathematical biology. Carrying out this project has convinced me to pursue my academic career in this direction; it provides me with so much joy to combine my knowledge about biology with my knowledge about mathematics and to see whereto this combination may lead.

I would also like to thank my family. I am very grateful to them for their trust, help and patience during my studies.

Summary

In this report I present the results from the mathematical analysis of a model neuronal network introduced by Ermentrout and Curtu [6], extended to two space dimensions. The model can be seen as a simple model of a cortical sheet that describes the firing rate activity of two populations of neurons coupled together, one excitatory that displays linear adaptation and the other one inhibitory. The dynamics of the activity is described by a system of nonlocal partial integro-differential equations in which a nonlinear sigmoidal-shaped firing rate function is included. The (synaptic) coupling between the neurons is characterized by local excitation and long range inhibition. Running numerical simulations with this model shows that a travelling hexagonal activity pattern is a stable solution of the model given certain sets of values for the parameters of the model. During this project I have investigated the mechanism behind the formation of these patterns as solutions of the model. The results from this investigation are presented in this report.

In order to investigate the mechanism I have used methods from nonlinear dynamical systems, pattern formation and bifurcation theory to analyze the model. I started by performing a linear stability analysis around the uniform quiescent state of the model (which is stable before the bifurcation points). From this analysis I could deduce the different types of bifurcation that could take place in the model. I decided to focus on the analysis of the Hopf bifurcation in order to investigate which types of spatio-temporal hexagonal pattern can be obtained in the model as a consequence of this type of bifurcation. Subsequently I performed a singular perturbation analysis to obtain the general solution of the model corresponding to spatio-temporal hexagonal activity patterns. Then I determined equilibrium solutions of this general solution which correspond with a travelling hexagonal activity pattern and a stationary, regularly oscillating hexagonal activity pattern. By finding these solutions through this analysis, it has become clear what the overall mechanism is behind their formation and why these solutions behave the way they do. Due to the fact that the stability of the trivial solution is lost at pure imaginary pairs of eigenvalues, spatio-temporal patterns can start bifurcating from the uniform quiescent state of the model. The exact shape of the function used to describe the coupling between the neurons in the model determines the shape of the activity patterns that can form in the model and the nonlinear sigmoidal-shaped firing rate function prevents the solutions from growing without bounds. The exact values of the parameters of the model determine the stability of the activity patterns.

It is interesting to note that the oscillating hexagonal activity pattern is a solution I've never found in numerical simulations. Due to a lack of time at present and the complexity of the problem at hand I have not been able to determine the exact stability conditions on the parameters of the model for each of the two found equilibrium solutions. However, an algorithm is presented to determine these conditions. With these stability conditions it must be possible to also find the oscillating pattern as a stable solution in numerical simulations with the model.

Contents

Chapter 1

Introduction

The neurons of organisms which have a nervous system are interconnected, together forming neuronal networks. Many areas of the brains of these species have a sheet-like architecture in which the neurons are connected horizontally in a particular way that is clearly not random. Neurons that respond preferentially to similar stimuli from the outside world, for example, are more strongly linked than those responding to different stimuli. The classic example of this phenomenon is the connection pattern of neurons in parts of the visual cortex [9]. These neurons respond to oriented bars of light and many of these cells have a preferred angle. The interesting thing is that experiments have shown that the neurons with a more similar angle preference are stronger linked than those with angle preferences further apart. Due to this non-random linkage pattern, which implies spatial organization of the connections between the neurons, it becomes possible to support the propagation of activity patterns (also known as activity waves) over cortical sheets and the existence of these waves has, therefore, been demonstrated in many systems over the last few decennia [3, 7]. These waves can be thought of as regions of the cortex in which the activity of the neurons is increased and the locations of these regions change over time in a regular fashion.

1.1 Motivation for the project

Previously, during the internship of my master's program "Brain and Cognitive Sciences", I have investigated, by using numerical simulations, whether or not a particular model with which I modelled a piece of cortical sheet could support the propagation of a particular (spatio-temporal) activity pattern as a stable solution [11]. If such a solution would exist, I could use it as part of a larger model with which I could provide support for a particular developmental theory which entails that the prenatal wiring of the neuronal interconnections in a particular brain system in rat embryos is dependent on activity waves which sweep over the prenatal cortex of these embryos.

The pattern I was looking for, was a semi-randomly translating hexagonal activity pattern (See Figure 2.3 to get an idea of what a (regularly) translating hexagonal activity pattern looks like). Although I found a translating hexagonal activity pattern as a stable solution, the found solution did not match the solution I was looking for. Unfortunately, the patterns always translated over the cortical sheet in a fixed direction with a fixed velocity of its constituting planar waves and whatever I tried, I could never change its direction, nor the velocity of its constituting planar waves (i.e. I always found a travelling hexagonal activity pattern). This was not what I was hoping to find because the model with this pattern as the stable solution does not provide support for the developmental theory. At that time it remained unclear to me why this type of solution exists in the type of model I used and why it behaves the way it does. Therefore I have carried out the current project in order to determine the mechanism behind the formation of these patterns as solutions in this type of model.

The model I have used for the mathematical analysis is a spatially extended version of a model developed Bard Ermentrout and Rodica Curtu [6]. This extended version of their model is nearly identical to the model I have used during the internship of my master's program. I am confident that results obtained from the analysis of the extended version of the model of Ermentrout and Curtu let themselves translate easily to insights for the model I have used during the internship.

The structure of the report is as follows. I start with a general description of the model of Ermentrout and Curtu. Next, I give a detailed description of the model that has been analyzed during this project. Then I delve into the actual analysis of this model after which I present my conclusions from carrying out this project.

1.2 The Ermentrout-Curtu model

The model of Ermentrout and Curtu is an one-dimensional model of interconnected cortical neurons on a finite or an infinite line and consists of two homogeneous populations of neurons, one excitatory (E) and the other one inhibitory (I). Classifying the population of cortical neurons into two sub populations is a reasonable thing to do, because the neurons of the cortex can be divided, in the simplest sense, into two types of cell, one excitatory and the other one inhibitory. They assumed that the excitatory neurons display linear adaptation. This is a phenomenon observed in the activity of neurons and entails a decline of their activity over time despite constant ongoing stimulation. This decline is a result of the constant stimulation, because it results in constant activity of these neurons which in turn causes them to fatigue. This makes it more and more difficult for them to stay active at the same level, hence the decline in their activity (hence, adaptation can be seen as a slow negative feedback mechanism). The inhibitory neurons in the model do not have a similar activity adaptation. These are reasonable asumptions, because most excitatory neurons have some form of adaptation while the inhibitory neurons generally do not have a similar activity adaptation [4].

Ermentrout and Curtu described the dynamics of the two populations by their firing rate activity (u_j with $j \in E, I$) and the adaptation by the variable A. The firing rate activity can be defined as the average number of action potentials per unit time. An action potential can be seen as a characteristic electrical pulse used by neurons to propagate signals into, through and from the brain. They assumed the spatial connectivity (J), also known as the synaptic coupling, to be all-to-all between the the excitatory neurons (J_{EE}), between the excitatory neurons and the inhibitory neurons (J_{IE}) and vice versa (J_{EI}). No interactions between the inhibitory neurons were included. For all of these interactions they assumed that the strength of the interactions decrease with the distance between the neurons according to a Gaussian curve with zero mean. Taken together, this resulted in the following general firing rate model

$$
\begin{aligned}
\tau_E \frac{\partial u_E}{\partial t}(x,t) &= -u_E(x,t) + F_E\left(J_{EE} * u_E(x,t) - J_{EI} * u_I(x,t) - gA\right), \\
\tau_I \frac{\partial u_I}{\partial t}(x,t) &= -u_I(x,t) + F_I\left(J_{IE} * u_E(x,t)\right), \\
\tau_A \frac{\partial A}{\partial t}(x,t) &= -A(x,t) + u_E(x,t).
\end{aligned}
\tag{1.1}
$$

τ_E, τ_I and τ_A represent respectively the time constants for the excitatory and inhibititory neurons and the time constant for the adaptation. The parameter g determines the gain of the adaptation, F_E and F_I are the firing-rate functions (i.e. the functions that translate the total input to a neuron through the interconnections into a change in the firing rate activity of the neuron) and the operator $J_{ij} * u_j$, with $i, j \in E, I$, is defined by the convolution

$$
J_{ij} * u_j(x,t) = \int J_{ij}(x-y) u_j(y,t) \, \mathrm{d}\, y.
$$

Next, Ermentrout and Curtu introduced one simplification to model (1.1). They assumed that the inhibition occurs on a must faster time scale than the excitation and that the firing rate activity for the inhibitory neurons is linear. This allowed them to replace the equation that decribes the dynamical evolution of the activity of the inhibitory neurons by its steady state (i.e. $u_I \approx J_{IE} * u_E$). Then they noticed that the convolution of two Gaussian functions with zero mean is still a Gaussian with zero mean. This implies

$$(J_{EE} * u_E - J_{EI} * u_I)(x,t) = (J_{EE} * u_E - J_{EI} * J_{IE} * u_E)(x,t) = (J_{EE} - J_{EI} * J_{IE}) * u_E(x,t) = J * u_E(x,t),$$

where the synaptic coupling $J(x)$ is a function of the difference of two Gaussian curves with zero mean. Due to these simplifications, model (1.1) could be reduced to a firing rate model for only one variable u, with the synaptic coupling defined by a Mexican hat function. This means that they assumed to have a network of neurons in which the interconnections are characterized by local excitation and long range (lateral) inhibition. This resulted in the following simplified model

$$\begin{aligned} \frac{\partial u}{\partial t}(x,t) &= -u(x,t) + F\left(\alpha J * u(x,t) - gv(x,t)\right), \\ \tau \frac{\partial v}{\partial t}(x,t) &= -v(x,t) + u(x,t). \end{aligned} \tag{1.2}$$

The variables $u(x,t)$ and $v(x,t)$ represent respectively the neuronal activity and the adaptation. The function F represents a firing rate function, the positive parameter α determines the strength of the synaptic coupling J between the neurons, the positive parameter g controls the gain of the adaptation and τ is the time constant.

Chapter 2

The description of the model under investigation

The model that I have analyzed, is the following

$$\begin{aligned} \frac{\partial u}{\partial t}(\mathbf{x},t) &= -u(\mathbf{x},t) + F\left(\alpha J * u(\mathbf{x},t) - gv(\mathbf{x},t)\right), \\ \tau\frac{\partial v}{\partial t}(\mathbf{x},t) &= -v(\mathbf{x},t) + u(\mathbf{x},t). \end{aligned} \tag{2.1}$$

The variables $u(\mathbf{x},t)$ and $v(\mathbf{x},t)$ represent the same as in the model of Ermentrout and Curtu (1.2). The only difference is that the neurons are situated on a two-dimensional neuronal sheet (Ω) so $\mathbf{x}$ is a two-dimensional (Euclidian) space coordinate ($\mathbf{x} = (x,y)^{\mathrm{T}}$). It is often assumed in analytical studies on neuronal models that the sides of neuronal sheets are infinite in length, but since I cannot consider an infinite domain in numerical simulations, I considered both a neuronal sheet with sides of (equal) finite length and an infinite neuronal sheet. Hence,

$$x, y \in \Omega = [-l,l] \times [-l,l] \quad \text{where} \quad l \in \{\mathbb{R}_{>0}, \infty\}. \tag{2.2}$$

With respect to the finite neuronal sheet I “glued” the opposite edges of the neuronal sheet together. This effectively creates a toroidal structure and implies periodic boundary conditions. The meaning of the parameters and the firing rate function are the same as in the model of Ermentrout and Curtu. Also the shape of the synaptic coupling was assumed to have the same properties as in the model of Ermentrout and Curtu, although changes due to the expansion to two space dimensions had to be taken into account. The precise shape of the synaptic coupling function used, a description of the operator $J * u(\mathbf{x},t)$ and the shape of the firing rate function used will be given in following sections.

2.1 The synaptic coupling function

The function I have used for the synaptic coupling is the following

$$J(x,y) = \frac{1}{\pi}\left(Aae^{-a\left(x^2+y^2\right)} - Bbe^{-b\left(x^2+y^2\right)}\right). \tag{2.3}$$

This function is a continuous, absolutely integrable function on the surface Ω and symmetric in the origin. The function has been constructed in such a way that nearby neurons are excited by active neurons while neurons further away from the active neurons are inhibited. In the case of an infinite neuronal network, the above defined coupling function is valid over the entire two-dimensional plane. In the case of a finite neuronal network the above defined coupling function is valid for $x, y \in [-l, l]$ where $l \in \mathbb{R}_{>0}$. Beyond the borders of this surface this function has to be "copied" over the two-dimensional plane so that the resulting function is double periodic of period $2l$. This is, of course, a necessity to accomodate the toroidal structure of the neuronal sheet. The parameters of this function satisfy

$$Aa \geq Bb > 0, \quad a > b > 0, \quad \sqrt{\frac{\ln\left(\frac{Bb}{Aa}\right)}{2(b-a)}} < l. \tag{2.4}$$

Taken together the above garantees that the assumption of short range excitation and long range inhibition is met independent of the length of a side of the neuronal sheet. Take a look at Figure 2.1(a) to see an example of what the function for the synaptic coupling typically looks like. The operator $J * u$ in model (2.1) represents the double convolution given by

$$J(x,y) * u(x,y,t) = \iint_{\Omega} J(x-v, y-w)u(v,w,t)\,\mathrm{d}\,v\,\mathrm{d}\,w. \tag{2.5}$$

The following Fourier transform is furthermore associated with the synaptic coupling

$$\hat{J}(\mathbf{k}) = \iint_{\Omega} J(\mathbf{x})e^{i\mathbf{k}\cdot\mathbf{x}}\,\mathrm{d}\,x\,\mathrm{d}\,y \tag{2.6}$$

where the variable $\mathbf{k}$ represents the two-dimensional wave vector ($\mathbf{k} = (k^1, k^2)^{\mathrm{T}}$). This transform will be used later on in the analysis. In the case of the function used for the synaptic coupling, application of (2.6) when working with an infinite neuronal network, results in

$$\hat{J}(k^1, k^2) = Ae^{\frac{-\left((k^1)^2+(k^2)^2\right)}{4a}} - Be^{\frac{-\left((k^1)^2+(k^2)^2\right)}{4b}}. \tag{2.7}$$

Application of (2.6) when working with a finite neuronal network, results in

$$\hat{J}(k^1, k^2) = \frac{1}{4}A\{V(a)\}e^{\frac{-\left((k^1)^2+(k^2)^2\right)}{4a}} - \frac{1}{4}B\{V(b)\}e^{\frac{-\left((k^1)^2+(k^2)^2\right)}{4b}}, \tag{2.8}$$

with

$$V(x) = P_1(x)Q_1(x) + P_2(x)Q_2(x) - P_1(x)Q_2(x) - P_2(x)Q_1(x),$$

and

$$P_1(x) = \operatorname{erf}\left(\frac{2lx + ik^1}{2\sqrt{x}}\right), \quad P_2(x) = \operatorname{erf}\left(\frac{-2lx + ik^1}{2\sqrt{x}}\right),$$
$$Q_1(x) = \operatorname{erf}\left(\frac{2lx + ik^2}{2\sqrt{x}}\right), \quad Q_2(x) = \operatorname{erf}\left(\frac{-2lx + ik^2}{2\sqrt{x}}\right).$$

Take a look at Figure 2.1(b) to see an example of the Fourier transform of the prototypical example of the function for the synaptic coupling. It should be noted that function $V(x)$ is real-valued for all $x, l \in \mathbb{R}_{>0}$ and $\mathbf{k} \in \mathbb{R}^2$. This is an important observation (which will become apparant later on in the analysis), because this implies that function (2.8) is a real-valued function. Looking at function (2.7) it of course clear that function (2.7) is also a real-valued function.

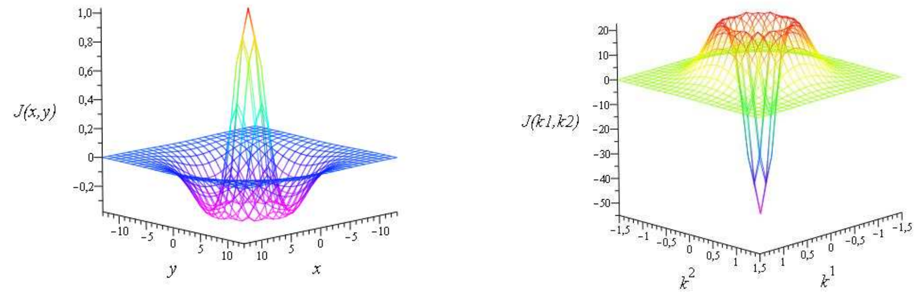

(a) $J(x, y)$ (b) $\hat{J}(k^1, k^2)$

Figure 2.1: (a) The synaptic coupling function $J(x, y)$ for $A = 70, B = 125, a = 0.1, b = 0.03$; (b) The Fourier transform $\hat{J}(k^1, k^2)$ of the synaptic coupling function depicted in (a).

2.2 The firing rate function

The function I have used as the firing rate function is the following sigmoidal function

$$F(u) = \frac{1 + e^{r\eta}}{r} \cdot \frac{1 - e^{-r\eta}}{1 + e^{-r(u-\eta)}}, \tag{2.9}$$

with r and η positive parameters. Take a look at Figure 2.2 to see an example of the firing rate function. This type of function is quite often used in this kind of modeling studies. If one assumes $\eta = 0$, for example, the above equation reduces to $F(u) = \frac{2}{r} \tanh\left(\frac{ru}{2}\right)$ and the use of a hyperbolic tangent for the firing rate function is common in the literature. Notice that function (2.9) satisfies

$$F(0) = 0 \quad \text{and} \quad F'(0) = 1. \tag{2.10}$$

This is important because both properties make the analysis of the model easier. The first property ensures that the uniform quiescent state of the model is the steady state of the model before the bifurcation points (i.e. $\bar{u} = 0, \bar{v} = 0$). The second property simplifies the analysis of model (2.1) when nonlinear terms of the model are taken into account.

It should be pointed out that the second property for the firing rate function is by no means essential as was pointed out by Curtu [5]. As long as $F'(0)$ is nonzero and positive, the results from the analysis will remain the same. If one assumes $F'(0) \neq 1$ then, by the change of variables, $u_{new} = u/F'(0)$, $v_{new} = v/F'(0)$, the change of the parameters $\alpha_{new} = F'(0)\alpha, g_{new} = F'(0)g$, and the change of the function $F_{new} = F/F'(0)$ a system topologically equivalent to system (2.1) is acquired where F_{new} satisfies the properties $F_{new}(0) = 0$ and $F'_{new}(0) = 1$. The exact shape of the firing rate function is also not essential because for the analysis I only need that the function $F(u)$ has continuous third derivatives at the origin. However, the model must use some sort of bounded function to prevent that solutions of the model can grow without bound.

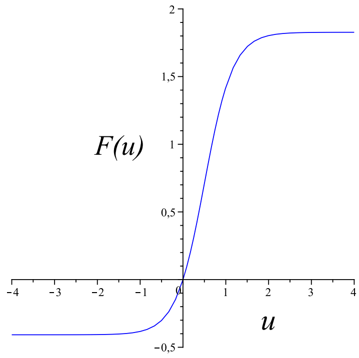

Figure 2.2: The firing rate function $F(u)$ for $r = 3, \eta = 0.5$.

2.3 Demonstration of a stable travelling hexagonal activity pattern in a numerical simulation

In order to assure myself that the spatially extended version of the model of Ermentrout and Curtu also harbors translating hexagonal activity patterns as a stable solution just like the model I have used during the internship of my master's program, I have implemented the model in MATLAB and I have run some simulations to see if I could find such translating solutions as a stable solution for a certain combination of parameter values of the model (see appendix C for the Matlab-code used for generating the numerical simulations).

Finding a stable translating hexagonal activity pattern in the extended version of the model of Ermentrout and Curtu with numerical simulations is not that hard to do. Take a look at Figure 2.3 to see that a stable hexagonal activity pattern which translates over the cortical sheet in a fixed direction with a fixed velocity of its constituting planar waves clearly exists in model (2.1). In the next chapters I present the mathematical analysis which sheds light onto why this type of solution of this type of model exists and behaves the way it does.

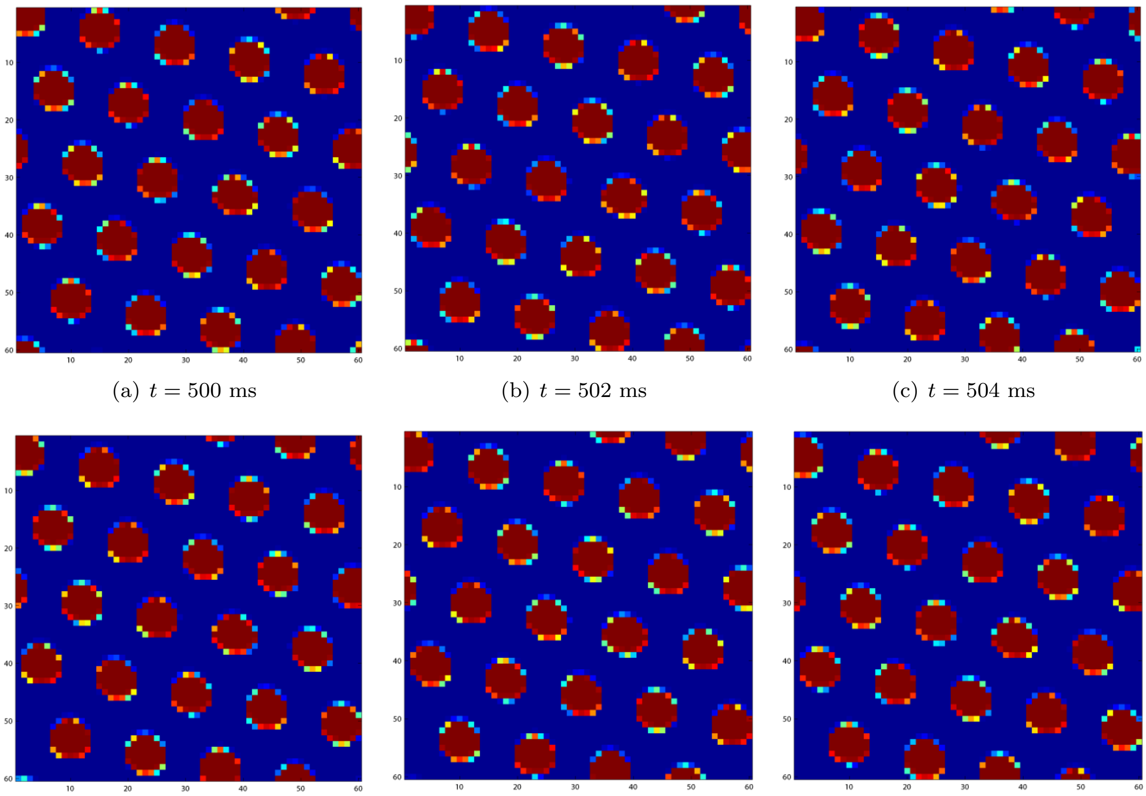

(a) $t = 500$ ms (b) $t = 502$ ms (c) $t = 504$ ms

(d) $t = 506$ ms (e) $t = 508$ ms (f) $t = 510$ ms

Figure 2.3: Results from a numerical simulation with model (2.1) for a cortical sheet consisting of 3600 neurons positioned on a square grid (60-by-60 neurons). The colors in the figure represent the amount of activity u of the neurons with dark red a high amount of activity and progressively cooler colors progressively lower amounts of activity. The translating hexagonal activity pattern is evident in the figures when one looks in succession at the sub figures from top left to bottom right. The direction of translation is south-south-west. For this simulation I have used the synaptic coupling function depicted in Figure 2.1(a), the firing rate function depicted in Figure 2.2 and the remaining parameters of the model have values $\alpha = 1, g = 4, \tau = 5$ ms. The Euler forward method with time step $dt = 0.1$ ms has been used as the method of intergation (See appendix C for the Matlab-code used for generating the numerical simulations).

Chapter 3

The linear stability analysis

I started the analysis of model (2.1) by performing a linear stability analysis in order to get an idea about the general behaviour of the steady state of the full nonlinear system beyond the possible bifurcation points. To this end I first linearized model (2.1) around the uniform quiescent state of the model:

$$
\begin{aligned}
\frac{\partial u}{\partial t} &= -u + (\alpha J * u - gv) + \frac{F''(0)}{2}(\alpha J * u - gv)^2 + \frac{F'''(0)}{6}(\alpha J * u - gv)^3 + \dots, \\
\frac{\partial v}{\partial t} &= \frac{-v}{\tau} + \frac{u}{\tau}.
\end{aligned}
\tag{3.1}
$$

Hence, the linear operator of the model is

$$
L_0 = \frac{\partial}{\partial t} - \begin{pmatrix} -1 + \alpha J * (\cdot) & -g \\ 1/\tau & -1/\tau \end{pmatrix}. \tag{3.2}
$$

Subsequently I performed the linear stability analysis around the uniform quiescent state of the model. I was looking for solutions of $L_0 U = \mathbf{0}$ with $U = (u, v)^{\mathrm{T}}$ that are bounded and have general shape $\xi(t)e^{i(\mathbf{k}\cdot\mathbf{x})}$. Application of the linear operator onto functions with this general shape results in

$$
\left[\frac{\mathrm{d}\,\xi}{\mathrm{d}\,t} - \hat{L}(\mathbf{k})\xi(t)\right] e^{i(\mathbf{k}\cdot\mathbf{x})} = \mathbf{0},
$$

where

$$
\hat{L}(\mathbf{k}) = \begin{pmatrix} -1 + \alpha\hat{J}(\mathbf{k}) & -g \\ 1/\tau & -1/\tau \end{pmatrix}. \tag{3.3}
$$

(Here I made use of (2.5) and (2.6)). When an infinite neuronal network is considered, the above is true for all $\mathbf{k} \in \mathbb{R}^2$ while the above holds for all $\mathbf{k} \in \pi\mathbb{Z}^2/l$ when a finite neuronal network is considered. Solving the ordinary differential equation $\mathrm{d}\,\xi/\,\mathrm{d}\,t = \hat{L}(\mathbf{k})\xi(t)$ yields two solutions $\xi_{1\mathbf{k}}e^{\lambda_{1\mathbf{k}}t}, \xi_{2\mathbf{k}}e^{\lambda_{2\mathbf{k}}t}$ where $\xi_{1,2\mathbf{k}}$ are two-dimensional complex vectors. Therefore the eigenfunctions of L_0 have the form

$$
\xi_{1,2\mathbf{k}}e^{\lambda_{1,2\mathbf{k}}t \pm i(\mathbf{k}\cdot\mathbf{x})} \quad \text{and} \quad \bar{\xi}_{1,2\mathbf{k}}e^{\bar{\lambda}_{1,2\mathbf{k}}t \mp i(\mathbf{k}\cdot\mathbf{x})}, \tag{3.4}
$$

where $\lambda_{1,2\mathbf{k}}$ are the eigenvalues of (3.3) for each wave vector $\mathbf{k}$ defined by

$$
\lambda_{1,2\mathbf{k}} = \frac{1}{2}\left(\operatorname{tr}\left(\hat{L}(\mathbf{k})\right) \pm \sqrt{\operatorname{tr}\left(\hat{L}(\mathbf{k})\right)^2 - 4\det\left(\hat{L}(\mathbf{k})\right)}\right), \tag{3.5}
$$

with

$$\operatorname{tr}\left(\hat{L}(\mathbf{k})\right) = -1 - 1/\tau + \alpha\hat{J}(\mathbf{k}),$$
$$\det\left(\hat{L}(\mathbf{k})\right) = \frac{1}{\tau}\left(-\alpha\hat{J}(\mathbf{k}) + 1 + g\right).$$

It should be noted once more that $\hat{J}(\mathbf{k})$ is a real-valued function for synaptic coupling functions of general form (2.3). I could conclude therefore that both the the trace and the determinant of (3.3) must be real-valued.

Before proceeding to the presentation of the results of the linear stability analysis, it is necessary to introduce the concept of the set of the most unstable wave vectors of the model. I have labeled this set $\mathbb{K}$ and it consists of wave vectors $\mathbf{k}_0^j = (k_0^{j,1}, k_0^{j,2})^{\mathrm{T}}$, i.e.

$$\mathbb{K} = \{\mathbf{k}_0^j\} \quad \text{with} \quad j = 1, 2, 3, \ldots \tag{3.6}$$

The wave vectors $\mathbf{k}_0^j$ are defined as the wave vectors $\mathbf{k}$ for which $\hat{J}(\mathbf{k})$ is maximized under the restriction $k_0^{j,1}, k_0^{j,2} \in \mathbb{R}$ in the case of an infinite neuronal network and under the restriction $k_0^{j,1}, k_0^{j,2} \in \pi\mathbb{Z}/l$ in the case of a finite neuronal network. This implies for function (2.3) with parameters satisfying (2.4) that the following holds for the wave vectors of set $\mathbb{K}$

$$\mathbf{k}_0^j \neq \mathbf{0}, \quad \hat{J}(\mathbf{k}_0^j) > 0 \quad \text{and} \quad |\mathbf{k}_0^j| = k_0, \quad \forall \mathbf{k}_0^j \in \mathbb{K}, \tag{3.7}$$

and in the case of an infinite neuronal network

$$\hat{J}(\mathbf{k}) < \hat{J}(\mathbf{k}_0^j), \quad \forall \mathbf{k} = (k^1, k^2)^{\mathrm{T}} \notin \mathbb{K} \text{ with } k^1, k^2 \in \mathbb{R}, \tag{3.8}$$

while in the case of a finite neuronal network

$$\hat{J}(\mathbf{k}) < \hat{J}(\mathbf{k}_0^j), \quad \forall \mathbf{k} = (k^1, k^2)^{\mathrm{T}} \notin \mathbb{K} \text{ with } k^1, k^2 \in \pi\mathbb{Z}/l. \tag{3.9}$$

It should be noted that the cardinality of set $\mathbb{K}$ is infinite in the case of an infinite neuronal network. This is a is a direct consequence of the (Euclidean) rotation symmetry of function (2.3). In the case of a finite neuronal network the cardinality of set $\mathbb{K}$ can be any multiple of four larger than or equal to four. The exact cardinality depends, of course, on the exact values chosen for the parameters of function (2.3). Note also that the wave vectors which belong to set $\mathbb{K}$ always appear by pairs with an angle of π radians between the wave vectors. These properties are a direct consequence of the (Euclidean) rotation symmetry of function (2.3). Finally also notice that the way in which the elements of set $\mathbb{K}$ are defined in combination with assumptions (3.7), (3.8) and (3.9), implies

$$\operatorname{tr}\left(\hat{L}(\mathbf{k})\right) < \operatorname{tr}\left(\hat{L}(\mathbf{k}_0^j)\right) \text{ and } \det\left(\hat{L}(\mathbf{k})\right) > \det\left(\hat{L}(\mathbf{k}_0^j)\right),$$

for all $\mathbf{k} \notin \mathbb{K}$ in the case of an infinite neuronal network and for all $\mathbf{k} \notin \mathbb{K}$ with $k^1, k^2 \in \pi\mathbb{Z}/l$ in the case of a finite neuronal network. Therefore, at the moment the uniform quiescent state loses its stability due to variation of bifurcation parameters one or two eigenvalues belonging to the wave vectors of set $\mathbb{K}$ cross the imaginary axis first and the functions from the basis for the nullspace of the linear operator L_0 with the wave vectors of set $\mathbb{K}$ form the basis for a center manifold that becomes the point of interest. The functions from the basis for the nullspace of the linear operator L_0 of the remaining wave vectors belong to a stable manifold.

Let me return now to the presentation of the results of the linear stability analysis. From (3.5) it follows that, if $\mathrm{tr}(\hat{L}(\mathbf{k})) < 0$ and $\det(\hat{L}(\mathbf{k})) > 0$ for all wave vectors $\mathbf{k}$ (i.e. $\alpha\hat{J}(\mathbf{k}) < 1+g$ and $\alpha\hat{J}(\mathbf{k}) < 1+1/\tau$), then all functions that form the basis for the nullspace of the linear operator L_0 correspond to a stable manifold and they exponentially decay in time to zero. Hence, the uniform quiescent state is asymptotically stable under these conditions. However, if the parameter(s) of model (2.1) is (are) varied beyond a bifurcation point, then there are three general ways in which the trivial solution can lose its stability. In terms of the parameters of the model, these three ways are the following:

1. the determinant of $\hat{L}(\mathbf{k})$ vanishes for the wave vectors of set $\mathbb{K}$ while the trace remains negative ($\alpha\hat{J}(\mathbf{k}_0^j) = 1 + g, g < 1/\tau$ for all $\mathbf{k}_0^j \in \mathbb{K}$). At this moment one real eigenvalue for each wave vector of set $\mathbb{K}$ crosses the imaginary axis ($\lambda_{1\mathbf{k}_0^j} = 0$), whereas $\lambda_{2\mathbf{k}_0^j} < 0$. At this moment the onset of stationary spatial activity patterns is expected. The exact type of pattern depends on the values of all the parameters of the model.

2. the trace of $\hat{L}(\mathbf{k})$ vanishes for the wave vectors of set $\mathbb{K}$ while the determinant remains positive ($\alpha\hat{J}(\mathbf{k}_0^j) = 1 + 1/\tau, g > 1/\tau$ for all $\mathbf{k}_0^j \in \mathbb{K}$). At this moment complex pairs of eigenvalues for each wave vector of set $\mathbb{K}$ cross the imaginary axis ($\lambda_{1,2\mathbf{k}_0^j} = \pm i\omega_0$) and the onset of spatio-temporal activity patterns is expected. The exact type of pattern depends on the values of all the parameters of the model.

3. both the determinant and the trace of $\hat{L}(\mathbf{k})$ vanish for the wave vectors of set $\mathbb{K}$ ($\alpha\hat{J}(\mathbf{k}_0^j) = 1 + 1/\tau, g = 1/\tau$ for all $\mathbf{k}_0^j \in \mathbb{K}$). At this moment the two eigenvalues for each wave vector of set $\mathbb{K}$ vanish simultaneously ($\lambda_{1,2\mathbf{k}_0^j} = 0$) which results in the onset of either spatio-temporal activity patterns or stationary spatial activity patterns. Which type of pattern appears, depends on the values of all the parameters of the model.

Chapter 4

The analysis of the linearized model including nonlinear terms

Subsequently I analyzed the linearized model including nonlinear terms (3.1) in the case that the stability of the uniform quiescent state is lost at pure imaginary pairs of eigenvalues to see if this could lead to the formation of new solutions consisting of spatio-temporal hexagonal activity patterns. I could also have focused on the condition where the stability of the trivial solution is lost at pairs of zero eigenvalues to see if this could lead to the formation of new solutions consisting of spatio-temporal hexagonal activity patterns. I know from the linear stability analysis that either of the two conditions can lead to the onset of spatio-temporal activity patterns. I, however, focused on the first condition and I left the analysis of the latter condition for another time.

I considered the parameter α (i.e. the strength of the synaptic coupling between the neurons) as the bifurcation parameter of model (2.1) and I defined the value of α for which it reaches its threshold value as α^*. The values of the parameters τ and g were assumed fixed in such a way that they meet the bifurcation conditions of (4.1). It should be noted that both the linear operator L_0 defined by (3.2) and the matrix $\hat{L}(\mathbf{k}_0^j)$ defined by (3.3) for all $\mathbf{k}_0^j \in \mathbb{K}$ were evaluated at $\alpha = \alpha^*$ on the remainder of the analysis.

Vanishing of the trace of matrix (3.3) results in $\lambda_{1,2\mathbf{k}_0^j} = \pm i\omega_0$ for all $\mathbf{k}_0^j \in \mathbb{K}$ and this vanishing of the trace takes place when the parameters of the model satisfy

$$\alpha^* \hat{J}(\mathbf{k}_0^j) = 1 + \frac{1}{\tau} \quad \text{and} \quad g > \frac{1}{\tau}. \tag{4.1}$$

A straightforward calculation shows that ω_0 satisfies

$$\omega_0 = \frac{\sqrt{-1 + g\tau}}{\tau}, \tag{4.2}$$

and the corresponding eigenvectors $\mathbf{\Phi}_0$ and $\bar{\mathbf{\Phi}}_0$ satisfy

$$\mathbf{\Phi}_0 = \left(\phi, \frac{\phi}{1 + i\sqrt{-1 + g\tau}}\right)^{\mathrm{T}} \quad \text{and} \quad \bar{\mathbf{\Phi}}_0 = \left(\phi, \frac{\phi}{1 - i\sqrt{-1 + g\tau}}\right)^{\mathrm{T}}. \tag{4.3}$$

4.1 Determination of the sought-after general solution of the model

I first determined which functions from the basis for the nullspace of the linear operator L_0 should form the basis for the center manifold in order for hexagonal activity patterns to start bifurcating from the uniform quiescent state at the moment the trace of matrix $\hat{L}(\mathbf{k}_0^j)$ vanishes (this approach was suggested by Paul Bressloff and colleagues [2]). From this the sought-after general solution could be deduced which subsequently allowed me to start looking for an equilibrium solution of this general solution consisting of a translating hexagonal activity pattern.

The functions that form the basis for the center manifold must satisfy

$$U(x,y,t) \approx U\left(x+\cos(\beta+\varphi)\frac{2\pi}{k_0}, y+\sin(\beta+\varphi)\frac{2\pi}{k_0}, t\right), \quad U(x,y,t) \approx U\left(x,y,t+\frac{2\pi}{\omega_0}\right) \tag{4.4}$$

for all $x, y \in \Omega$, for all $t \in \mathbb{R}$, for $\beta \in [0, \pi/3\rangle$, for $\varphi \in \{n\pi/3 \mid n = \{0,1,2,3,4,5\}\}$ with $U = (u,v)^{\mathrm{T}}$ and k_0 defined by (3.7). It should be mentioned that the angle β is a random, but fixed angle and it merely determines the overall orientation of the hexagonal activity pattern against the x-axis. In the case of a finite neuronal network with $l \in \mathbb{R}_{>0}$ these functions must furthermore satisfy

$$U(-l, -l < y < l, t) = U(l, -l < y < l, t) \quad \text{and} \quad U(-l < x < l, -l, t) = U(-l < x < l, l, t) \tag{4.5}$$

for all $t \in \mathbb{R}$. This latter assumption is a direct consequence of the periodic boundary conditions which are a result of “glueing together” the edges of the neuronal sheet. The functions that satisfy the above assumptions are exactly the type of functions that are doubly periodic with respect to a hexagonal lattice $\mathcal{L}$ and therefore should form the basis for the center manifold.

Due to a restriction of the solution space to functions that fullfil the above, considerable difficulties are side-stepped. As was stated in the previous chapter, (Euclidean) rotation symmetry of the function defined for the synaptic coupling (i.e. function (2.3)) implies that set $\mathbb{K}$ contains an infinite number of elements in the case of an infinite neuronal network. In the case of a finite neuronal network the set $\mathbb{K}$ contains at least four elements, but this number is often larger. This implies that the basis for the center manifold is infinite-dimensional in the case of an infinite neuronal network and (very) high-dimensional in the case of a finite neuronal network when no restrictions are imposed on the sought-after patterns as possible solutions for the model. This lack of restrictions makes a full analysis of linearized model problematic. However, the symmetries of the restricted problem change from the Euclidean symmetry in two ways. First, only a finite number of rotations and reflections remain as symmetries that preserve the hexagonal lattice (which in this case implies the rotations and reflections of the dihedral group $\mathbb{D}_6$). Second, translations act on the restricted problem modulo the hexagonal lattice: that is, translations act as a torus $\mathbb{T}^2$. Therefore, the symmetry group of the hexagonal lattice problem is $\Gamma_{\mathcal{L}} = \mathbb{D}_6 + \mathbb{T}^2$. Hence, it follows from double periodicity that the basis for the center manifold of the restricted problem is twelve-dimensional and consists of functions

$$\mathbf{\Phi}_0 e^{i(\omega_0 t \pm \mathbf{k}_0^j \cdot \mathbf{x})} \quad \text{and} \quad \bar{\mathbf{\Phi}}_0 e^{-i(\omega_0 t \pm \mathbf{k}_0^j \cdot \mathbf{x})} \tag{4.6}$$

with $\mathbf{k}_0^j \in \mathbb{K}$ for $j = 1, 2, 3$ under the restriction that the angles between the different wave vectors are $2\pi/3$ radians.

By subsequently using a singular perturbation analysis on the linearized model including nonlinear terms (3.1) I was able to obtain the sought-after general solution of model (2.1):

$$U(\mathbf{x},t) \approx 2\mathrm{Re}\Big\{\mathbf{\Phi}_0\Big[Z_1(t)e^{i(\omega_0 t+\mathbf{k}_0^1\cdot\mathbf{x})}+Z_2(t)e^{i(\omega_0 t+\mathbf{k}_0^2\cdot\mathbf{x})}+Z_3(t)e^{i(\omega_0 t+\mathbf{k}_0^3\cdot\mathbf{x})}+ \\ W_1(t)e^{i(\omega_0 t-\mathbf{k}_0^1\cdot\mathbf{x})}+W_2(t)e^{i(\omega_0 t-\mathbf{k}_0^2\cdot\mathbf{x})}+W_3(t)e^{i(\omega_0 t-\mathbf{k}_0^3\cdot\mathbf{x})}\Big]\Big\} \tag{4.7}$$

with $\mathbf{k}_0^j \in \mathbb{K}$ for $j = 1,2,3$ under the restriction that the angles between the different wave vectors are $2\pi/3$ radians. The coefficients $Z_j(t), W_j(t)$ for $j = 1,2,3$ satisfy the system of ordinary differential equations

$$\begin{cases} Z_j'(t) = a^j Z_j(t) + b^j Z_j(t)|Z_j(t)|^2 + c^j Z_j(t)|W_j(t)|^2 + Z_j(t)\displaystyle\sum_{l=1}^{3}\left(d^{j,l}|W_l(t)|^2\right) + \\ \qquad Z_j(t)\displaystyle\sum_{\substack{m=1\\ m\neq j}}^{3}\left(e^{j,m}|Z_m(t)|^2\right) + \bar{W}_j(t)\displaystyle\sum_{\substack{n=1\\ n\neq j}}^{3}\left(f^{j,n}Z_n(t)W_n(t)\right), \\ W_j'(t) = a^j W_j(t) + b^j W_j(t)|W_j(t)|^2 + c^j W_j(t)|Z_j(t)|^2 + W_j(t)\displaystyle\sum_{l=1}^{3}\left(d^{j,l}|Z_l(t)|^2\right) + \\ \qquad W_j(t)\displaystyle\sum_{\substack{m=1\\ m\neq j}}^{3}\left(e^{j,m}|W_m(t)|^2\right) + \bar{Z}_j(t)\displaystyle\sum_{\substack{n=1\\ n\neq j}}^{3}\left(f^{j,n}Z_n(t)W_n(t)\right). \end{cases} \tag{4.8}$$

The details of the singular perturbation analysis are given in appendix A and the definitions for the coefficients of (4.8) are given in (A.26).

4.2 Determination of equilibrium solutions for the sought-after general solution of the model

After the determination of the sought-after general solution of the model, I could start looking for equilibrium solutions of this general solution and I could start trying to determine the qualitative picture of the bifurcating patterns that are associated with these equilibrium solutions. Finding equilibrium solutions for the sought-after general solution boils down to finding equilibrium solutions for the system of ordinary differential equations from (4.8).

In order to find these, I started by writing this system in polar coordinates. Therefore I defined $Z_j = r_j e^{i\theta_j}$ and $W_j = R_j e^{i\phi_j}$ for $j = 1, 2, 3$. Then system (4.8) is equivalent to the system

$$\begin{cases} r_j'(t) = a_1^j r_j(t) + b_1^j (r_j(t))^3 + c_1^j r_j(t)(R_j(t))^2 + r_j(t) \sum\limits_{l=1}^{3} \left(d_1^{j,l} (R_l(t))^2 \right) + \\ \qquad r_j(t) \sum\limits_{\substack{m=1 \\ m \neq j}}^{3} \left(e_1^{j,m} (r_m(t))^2 \right) + R_j(t) \sum\limits_{\substack{n=1 \\ n \neq j}}^{3} \left(f_1^{j,n} r_n(t) R_n(t) e^{i(\theta_n(t)+\phi_n(t)-\theta_j(t)-\phi_j(t))} \right), \\ R_j'(t) = a_1^j R_j(t) + b_1^j (R_j(t))^3 + c_1^j R_j(t)(r_j(t))^2 + R_j(t) \sum\limits_{l=1}^{3} \left(d_1^{j,l} (r_l(t))^2 \right) + \\ \qquad R_j(t) \sum\limits_{\substack{m=1 \\ m \neq j}}^{3} \left(e_1^{j,m} (R_m(t))^2 \right) + r_j(t) \sum\limits_{\substack{n=1 \\ n \neq j}}^{3} \left(f_1^{j,n} r_n(t) R_n(t) e^{i(\theta_n(t)+\phi_n(t)-\theta_j(t)-\phi_j(t))} \right), \\ \theta_j'(t) = a_2^j + b_2^j (r_j(t))^2 + c_2^j (R_j(t))^2 + \sum\limits_{l=1}^{3} \left(d_2^{j,l} (R_l(t))^2 \right) + \\ \qquad \sum\limits_{\substack{m=1 \\ m \neq j}}^{3} \left(e_2^{j,m} (r_m(t))^2 \right) + R_j(t)(r_j(t))^{-1} \sum\limits_{\substack{n=1 \\ n \neq j}}^{3} \left(f_2^{j,n} r_n(t) R_n(t) e^{i(\theta_n(t)+\phi_n(t)-\theta_j(t)-\phi_j(t))} \right), \\ \phi_j'(t) = a_2^j + b_2^j (R_j(t))^2 + c_2^j (r_j(t))^2 + \sum\limits_{l=1}^{3} \left(d_2^{j,l} (r_l(t))^2 \right) + \\ \qquad \sum\limits_{\substack{m=1 \\ m \neq j}}^{3} \left(e_2^{j,m} (R_m(t))^2 \right) + r_j(t)(R_j(t))^{-1} \sum\limits_{\substack{n=1 \\ n \neq j}}^{3} \left(f_2^{j,n} r_n(t) R_n(t) e^{i(\theta_n(t)+\phi_n(t)-\theta_j(t)-\phi_j(t))} \right), \end{cases} \tag{4.9}$$

for $j = 1, 2, 3$. Finding equilibrium solutions for this system of ordinary differential equations is cumbersome because of the term $e^{i(\theta_n(t)+\phi_n(t)-\theta_j(t)-\phi_j(t))}$ in the above equations. Fortunately I thought of a small trick that I could apply which made the search for equilibrium solutions for this system easier. The nice thing is also that I could justify its application in retrospect.

Curtu and Ermentrout investigated what types of spatial and spatio-temporal pattern could stabilize in their model (1.2) [6]. They found that both travelling (i.e. regularly translating) and regularly oscillating wave patterns are stable (spatio-temporal) solutions given the right conditions of the model (these patterns cannot simultaneously be stable so at a Hopf bifurcation, for example, either one of the two stabilizes). Therefore I thought that similar spatio-temporal patterns expanded to two space dimensions (i.e. a travelling hexagonal activity pattern and a stationary, regulalry oscillating hexagonal activity pattern) might also stabilize in the current model under investigation (i.e. model (2.1). Actually I already know from numerical simulations with the model that a travelling hexagonal activity pattern does indeed stabilize in the model (see Figure 2.3 for an example).

Now in order for a stationary, regularly oscillating hexagonal activity pattern to oscillate with a constant frequency, the following must hold: $\bar{\theta}_1 \approx \bar{\phi}_1 \approx \bar{\theta}_2 \approx \bar{\phi}_2 \approx \bar{\theta}_3 \approx \bar{\phi}_3$. Regularly translating hexagonal patterns on the other hand can only travel with a constant velocity if the following holds: $\bar{\theta}_1 \approx \bar{\theta}_2 \approx \bar{\theta}_3$ and $\bar{\phi}_1 \approx \bar{\phi}_2 \approx \bar{\phi}_3$. Assuming this allows me to take $e^{i(\bar{\theta}_n(t)+\bar{\phi}_n(t)-\bar{\theta}_j(t)-\bar{\phi}_j(t))} = 1$ when looking for equilibrium solutions and after applying this simplification, it becomes relatively easy to find equilibrium solutions for the system from (4.9).

4.2.1 The travelling hexagonal activity pattern

I found two equilibrium solutions that corrspond to travelling hexagonal activity patterns by assuming $\bar{r}_1 = \bar{r}_2 = \bar{r}_3 = 0$ or $\bar{R}_1 = \bar{R}_2 = \bar{R}_3 = 0$ (and hence also $\bar{\theta}_1 \approx \bar{\theta}_2 \approx \bar{\theta}_3$ and $\bar{\phi}_1 \approx \bar{\phi}_2 \approx \bar{\phi}_3$). Assuming $\bar{r}_1 = \bar{r}_2 = \bar{r}_3 = 0$ implies the following for the equilibrium values of R_1, R_2 and R_3:

$$\begin{aligned}
\bar{R}_1 &= \sqrt{\frac{a_1^1 e_1^{32} e_1^{23} - a_1^1 b_1^2 b_1^3 + a_1^2 b_1^3 e_1^{12} - a_1^3 e_1^{12} e_1^{23} + a_1^3 b_1^2 e_1^{13} - a_1^2 e_1^{13} e_1^{31}}{b_1^1 b_1^2 b_1^3 - b_1^1 e_1^{23} e_1^{32} - b_1^2 e_1^{13} e_1^{31} - b_1^3 e_1^{12} e_1^{21} + e_1^{32} e_1^{21} e_1^{13} + e_1^{31} e_1^{12} e_1^{23}}}, \\
\bar{R}_2 &= \sqrt{\frac{a_1^2 e_1^{31} e_1^{13} - a_1^2 b_1^1 b_1^3 + a_1^3 b_1^1 e_1^{23} - a_1^3 e_1^{21} e_1^{13} + a_1^1 b_1^3 e_1^{21} - a_1^1 e_1^{23} e_1^{31}}{b_1^1 b_1^2 b_1^3 - b_1^1 e_1^{23} e_1^{32} - b_1^2 e_1^{13} e_1^{31} - b_1^3 e_1^{12} e_1^{21} + e_1^{32} e_1^{21} e_1^{13} + e_1^{31} e_1^{12} e_1^{23}}}, \\
\bar{R}_3 &= \sqrt{\frac{a_1^3 e_1^{21} e_1^{12} - a_1^3 b_1^1 b_1^2 + a_1^2 b_1^1 e_1^{32} - a_1^2 e_1^{31} e_1^{12} + a_1^1 b_1^2 e_1^{31} - a_1^1 e_1^{32} e_1^{21}}{b_1^1 b_1^2 b_1^3 - b_1^1 e_1^{23} e_1^{32} - b_1^2 e_1^{13} e_1^{31} - b_1^3 e_1^{12} e_1^{21} + e_1^{32} e_1^{21} e_1^{13} + e_1^{31} e_1^{12} e_1^{23}}}.
\end{aligned} \tag{4.10}$$

Here it is assumed that the coefficients of the system of ordinary differential equations from (4.9) have values such that the above equilibrium values are real. It should be noted that the equilibrium values of R_1, R_2 and R_3 are all equal. This becomes apparent after a careful examination of all the parameters that constitute the equilibrium values (see (A.26)) and therefore I introduce

$$S := \bar{R}_1 = \bar{R}_2 = \bar{R}_3. \tag{4.11}$$

Assuming $\bar{R}_1 = \bar{R}_2 = \bar{R}_3 = 0$ results in finding the same equilibrium values for r_1, r_2 and r_3 as for R_1, R_2 and R_3 in (4.10) with $\bar{R}_1$ replaced by $\bar{r}_1$, $\bar{R}_2$ replaced by $\bar{r}_2$ and $\bar{R}_3$ replaced by $\bar{r}_3$ (and therefore the following als holds: $\bar{r}_1 = \bar{r}_2 = \bar{r}_3 = S$). The equilibrium solutions for θ_j and ϕ_j in the case of $\bar{r}_1 = \bar{r}_2 = \bar{r}_3 = 0$ are

$$\begin{aligned}
\bar{\theta}_j(t) &= \left(a_2^j + c_2^j S^2 + \sum_{l=1}^{3} \left(d_2^{j,l} \right) S^2 + \sum_{\substack{n=1 \\ n \neq j}}^{3} \left(f_2^{j,n} \right) S^2 \right) t, \\
\bar{\phi}_j(t) &= \left(a_2^j + b_2^j S^2 + \sum_{\substack{m=1 \\ m \neq j}}^{3} \left(e_2^{j,m} \right) S^2 \right) t,
\end{aligned} \tag{4.12}$$

for $j = 1, 2, 3$. When it is assumed that $\bar{R}_1 = \bar{R}_2 = \bar{R}_3 = 0$, then the equilibrium solutions for θ_j for $j = 1, 2, 3$ are the same as in (4.12) with $\bar{\phi}_j(t)$ replaced by $\bar{\theta}_j(t)$ and $\bar{\theta}_j(t)$ replaced by $\bar{\phi}_j(t)$.

Taken together the above found equilibrium solutions for the system of ordinary differential equations from (4.9) imply that model (2.1) has a solution that can be approximated by

$$U(\mathbf{x},t) \approx 2S \cdot \mathrm{Re}\left\{ \mathbf{\Phi}_0 \left[e^{i(\omega_0 t \pm \mathbf{k}_0^1 \cdot \mathbf{x})} + e^{i(\omega_0 t \pm \mathbf{k}_0^2 \cdot \mathbf{x})} + e^{i(\omega_0 t \pm \mathbf{k}_0^3 \cdot \mathbf{x})} \right] \right\} \tag{4.13}$$

for $\alpha > \alpha^*$, sufficiently close to α^* with the angles between the different wave vectors equal to $2\pi/3$ radians and with ω_0 and $\mathbf{\Phi}_0$ defined respectively by (4.2) and (4.3). Here I made use of the fact that $\omega_0 t + \bar{\theta}_j(t) \approx \omega_0 t$ and $\omega_0 t + \bar{\phi}_j(t) \approx \omega_0 t$ at $\alpha \to \alpha^*$. This follows from the fact that all terms on the right-hand side in (4.12) contain the parameter a_1^j or a_2^j in their numerators. Looking at (A.26), it becomes apparent that these parameters are comparatively small at $\alpha \to \alpha^*$. Hence $\omega_0 t + \bar{\theta}_j(t) \approx \omega_0 t$ and $\omega_0 t + \bar{\phi}_j(t) \approx \omega_0 t$.

The solution from (4.13) does indeed clearly represent a travelling hexagonal activity pattern and the velocity of the individual travelling planar waves that constitute the travelling hexagonal activity pattern is $c = \pm\omega_0/k_0$. Notice that the assumptions $\bar{\theta}_1 \approx \bar{\theta}_2 \approx \bar{\theta}_3$ and $\bar{\phi}_1 \approx \bar{\phi}_2 \approx \bar{\phi}_3$ were justified. This follows from (4.12) and looking carefully at the parameters that constitute the coefficients of the equilibrium solutions of (4.12).

4.2.2 The stationary, regularly oscillating hexagonal activity pattern

I found another equilibrium solution that corresponds to a stationary, regularly oscillating hexagonal activity pattern by assuming $\bar{r}_1 = \bar{R}_1$, $\bar{r}_2 = \bar{R}_2$ and $\bar{r}_3 = \bar{R}_3$ (and hence also $\bar{\theta}_1 \approx \bar{\phi}_1 \approx \bar{\theta}_2 \approx \bar{\phi}_2 \approx \bar{\theta}_3 \approx \bar{\phi}_3$). This implies the following for the equilibrium values of r_1, r_2, r_3, R_1, R_2 and R_3:

$$\begin{aligned}
\bar{r}_1 = \bar{R}_1 = E\Big[& a_1^1 \left(d_1^{23}+e_1^{23}+f_1^{23}\right)\left(d_1^{32}+e_1^{32}+f_1^{32}\right) - a_1^1 \left(b_1^2+c_1^2+d_1^{22}\right)\left(b_1^3+c_1^3+d_1^{33}\right) + \\
& a_1^2 \left(d_1^{12}+e_1^{12}+f_1^{12}\right)\left(b_1^3+c_1^3+d_1^{33}\right) - a_1^2 \left(d_1^{13}+e_1^{13}+f_1^{13}\right)\left(d_1^{32}+e_1^{32}+f_1^{32}\right) + \\
& a_1^3 \left(d_1^{13}+e_1^{13}+f_1^{13}\right)\left(b_1^2+c_1^2+d_1^{22}\right) - a_1^3 \left(d_1^{12}+e_1^{12}+f_1^{12}\right)\left(d_1^{23}+e_1^{23}+f_1^{23}\right)\Big]^{\frac{1}{2}}, \\
\bar{r}_2 = \bar{R}_2 = E\Big[& a_1^1 \left(d_1^{21}+e_1^{21}+f_1^{21}\right)\left(b_1^3+c_1^3+d_1^{33}\right) - a_1^1 \left(d_1^{23}+e_1^{23}+f_1^{23}\right)\left(d_1^{31}+e_1^{31}+f_1^{31}\right) + \\
& a_1^2 \left(d_1^{13}+e_1^{13}+f_1^{13}\right)\left(d_1^{31}+e_1^{31}+f_1^{31}\right) - a_1^2 \left(b_1^1+c_1^1+d_1^{11}\right)\left(b_1^3+c_1^3+d_1^{33}\right) + \\
& a_1^3 \left(b_1^1+c_1^1+d_1^{11}\right)\left(d_1^{23}+e_1^{23}+f_1^{23}\right) - a_1^3 \left(d_1^{13}+e_1^{13}+f_1^{13}\right)\left(d_1^{21}+e_1^{21}+f_1^{21}\right)\Big]^{\frac{1}{2}}, \\
\bar{r}_3 = \bar{R}_3 = E\Big[& a_1^1 \left(b_1^2+c_1^2+d_1^{22}\right)\left(d_1^{31}+e_1^{31}+f_1^{31}\right) - a_1^1 \left(d_1^{21}+e_1^{21}+f_1^{21}\right)\left(d_1^{32}+e_1^{32}+f_1^{32}\right) + \\
& a_1^2 \left(b_1^1+c_1^1+d_1^{11}\right)\left(d_1^{32}+e_1^{32}+f_1^{32}\right) - a_1^2 \left(d_1^{12}+e_1^{12}+f_1^{12}\right)\left(d_1^{31}+e_1^{31}+f_1^{31}\right) + \\
& a_1^3 \left(d_1^{12}+e_1^{12}+f_1^{12}\right)\left(d_1^{21}+e_1^{21}+f_1^{21}\right) - a_1^3 \left(b_1^1+c_1^1+d_1^{11}\right)\left(b_1^2+c_1^2+d_1^{22}\right)\Big]^{\frac{1}{2}},
\end{aligned} \tag{4.14}$$

with

$$\begin{aligned}
E = \Big[& \left(b_1^1+c_1^1+d_1^{11}\right)\left(b_1^2+c_1^2+d_1^{22}\right)\left(b_1^3+c_1^3+d_1^{33}\right) + \\
& \left(d_1^{12}+e_1^{12}+f_1^{12}\right)\left(d_1^{23}+e_1^{23}+f_1^{23}\right)\left(d_1^{31}+e_1^{31}+f_1^{31}\right) + \\
& \left(d_1^{13}+e_1^{13}+f_1^{13}\right)\left(d_1^{21}+e_1^{21}+f_1^{21}\right)\left(d_1^{32}+e_1^{32}+f_1^{32}\right) - \\
& \left(b_1^1+c_1^1+d_1^{11}\right)\left(d_1^{23}+e_1^{23}+f_1^{23}\right)\left(d_1^{32}+e_1^{32}+f_1^{32}\right) - \\
& \left(d_1^{12}+e_1^{12}+f_1^{12}\right)\left(d_1^{21}+e_1^{21}+f_1^{21}\right)\left(b_1^3+c_1^3+d_1^{33}\right) - \\
& \left(d_1^{13}+e_1^{13}+f_1^{13}\right)\left(b_1^2+c_1^2+d_1^{22}\right)\left(d_1^{31}+e_1^{31}+f_1^{31}\right)\Big]^{-\frac{1}{2}}.
\end{aligned}$$

Here it is again assumed that the coefficients of the system of ordinary differential equations from (4.9) have values such that the above equilibrium values are real. It should be noted that the equilibrium values of R_1, R_2 and R_3 are all equal (and therefore also equal to r_1, r_2 and r_3). This becomes once more apparent after a careful examination of all the parameters that constitute the equilibrium values (see (A.26)) and therefore I introduce

$$T := \bar{r}_1 = \bar{R}_1 = \bar{r}_2 = \bar{R}_2 = \bar{r}_3 = \bar{R}_3. \tag{4.15}$$

The equilibrium solutions for θ_j and ϕ_j are

$$\bar{\theta}_j(t) = \bar{\phi}_j(t) = \left(a_2^j + (b_2^j + c_2^j)T^2 + \sum_{l=1}^{3} \left(d_2^{j,l}\right) T^2 + \sum_{\substack{m=1 \\ m \neq j}}^{3} \left(e_2^{j,m}\right) T^2 + \sum_{\substack{n=1 \\ n \neq j}}^{3} \left(f_2^{j,n}\right) T^2 \right) t \tag{4.16}$$

for $j = 1, 2, 3$.

Taken together the above found equilibrium solution for the system of ordinary differential equations from (4.9) imply that model (2.1) has a solution that can be approximated by

$$U(\mathbf{x}, t) \approx 4T \left[\cos(\mathbf{k}_0^1 \cdot \mathbf{x}) + \cos(\mathbf{k}_0^2 \cdot \mathbf{x}) + \cos(\mathbf{k}_0^3 \cdot \mathbf{x})\right] \cdot \mathrm{Re}\left\{\mathbf{\Phi}_0 e^{i\omega_0 t}\right\} \tag{4.17}$$

for $\alpha > \alpha^*$, sufficiently close to α^* with the angles between the different wave vectors equal to $2\pi/3$ radians and with ω_0 and $\mathbf{\Phi}_0$ defined respectively by (4.2) and (4.3). Here I once more made use of the fact that $\omega_0 t + \bar{\theta}_j(t) \approx \omega_0 t$ and $\omega_0 t + \bar{\phi}_j(t) \approx \omega_0 t$ at $\alpha \to \alpha^*$. This follows from the fact that all terms on the right-hand side in (4.16) contain the parameter a_1^j or a_2^j in their numerators. Looking at (A.26), it becomes apparent that these parameters are comparatively small at $\alpha \to \alpha^*$. Hence $\omega_0 t + \bar{\theta}_j(t) \approx \omega_0 t$ and $\omega_0 t + \bar{\phi}_j(t) \approx \omega_0 t$.

The solution from (4.17) does indeed clearly represent a stationary, regularly oscillating hexagonal activity pattern. The individual standing planar waves that constitute the activity pattern are periodic in space with spatial frequency k_0, and periodic in time with temporal frequency ω_0. Notice that the assumption $\bar{\theta}_1 \approx \bar{\phi}_1 \approx \bar{\theta}_2 \approx \bar{\phi}_2 \approx \bar{\theta}_3 \approx \bar{\phi}_3$ was justified. This follows from (4.16) and looking carefully at the parameters that constitute the coefficients of the equilibrium solutions of (4.16).

4.3 On the stability of the found equilibrium solutions

As the last step of the analysis I wished to determine the stability conditions on the coefficients of the system of ordinary differential equations from (4.9) for the above found equilibrium solutions, assuming that these conditions do exist. However, this is a lot of work as a consequence of the large number of coeffcients in the system of ordinary differential equations from (4.9), the dimensionality of the system, the complexity of the equilibrium solutions and the complexity of the coefficients themselves (see (A.26) for the definitions of these coeffcients). Unfortunately I don't have the time anymore at present to carry out this part of the analysis. Therefore I cannot present a complete derivation of these conditions here, but I will present an algorithm that can be used to determine these conditions.

Determination of the stability conditions on the coefficients of the system of ordinary differential equations from (4.9) for the above found equilibrium solutions boils down to a determination of the conditions on the coeffcents such that the eigenvalues of the linearized system of $r_j(t)$ and $R_j(t)$ for $j = 1, 2, 3$ around the equilibrium solutions are all situated in the left half of the complex plane. Hence the first step of the procedure consists of linearizing the following system

$$\begin{cases} r_j'(t) = a_1^j r_j(t) + b_1^j (r_j(t))^3 + c_1^j r_j(t)(R_j(t))^2 + r_j(t) \sum_{l=1}^{3} \left(d_1^{j,l} (R_l(t))^2 \right) + \\ \qquad r_j(t) \sum_{\substack{m=1 \\ m \neq j}}^{3} \left(e_1^{j,m} (r_m(t))^2 \right) + R_j(t) \sum_{\substack{n=1 \\ n \neq j}}^{3} \left(f_1^{j,n} r_n(t) R_n(t) e^{i(\theta_n(t)+\phi_n(t)-\theta_j(t)-\phi_j(t))} \right), \\ R_j'(t) = a_1^j R_j(t) + b_1^j (R_j(t))^3 + c_1^j R_j(t)(r_j(t))^2 + R_j(t) \sum_{l=1}^{3} \left(d_1^{j,l} (r_l(t))^2 \right) + \\ \qquad R_j(t) \sum_{\substack{m=1 \\ m \neq j}}^{3} \left(e_1^{j,m} (R_m(t))^2 \right) + r_j(t) \sum_{\substack{n=1 \\ n \neq j}}^{3} \left(f_1^{j,n} r_n(t) R_n(t) e^{i(\theta_n(t)+\phi_n(t)-\theta_j(t)-\phi_j(t))} \right), \end{cases} \tag{4.18}$$

for $j = 1, 2, 3$ around the equilibrium solutions (4.10) and (4.12) or (4.14) and (4.16). Fortunately the equilibrium solutions of (4.12) and (4.16) for $\bar{\theta}_j$ and $\bar{\phi}_j$ are such that $e^{i(\theta_n(t)+\phi_n(t)-\theta_j(t)-\phi_j(t))} = 1$ holds for both linearizations. This simplifies the linearized systems slightly. The characteristic polynomials of the linearized systems need to be determined next. The linearized systems are six-dimensional systems so the characteristic polynomials for these systems are monic sextic polynomials (with indeed very complicated expressions for the coefficients of these polynomials). The stability conditions on the coefficients of the system of ordinary differential equations from (4.18) can be determined now such that the eigenvalues of the linearized system of $r_j(t)$ and $R_j(t)$ for $j = 1, 2, 3$ around the equilibrium solutions are all situated in the left half of the complex plane by finding the conditions on these coefficients for which the roots of the monic sextic polynomials are all positioned in the left half of the complex plane.

Finding these conditions is not at all straightforward, but there is a relatively easy solution. Recently Huang and Cheng have published an article in which they present a clear method to determine the necessary and sufficient conditions on the coefficients of general monic sextic polynomials with six real-valued coefficients such that the polynomial does not have any positive roots [10]. The characteristic polynomials for the linearized systems under consideration have real-valuad coefficients, because the coefficients in the system of ordinary differential equations from (4.9) are real-valued and the first constriction imposed on the coefficients in this system was that they were assumed to have values such that the equilibrium solutions would be real-valued. Hence, the method of Huang and Cheng can be used to determine the stability conditions on the coefficients of the system of ordinary differential equations from (4.9) for the above found equilibrium solutions.

Carrying out the above outlined procedure by hand is of course nearly impossible, but with an implementation in a computer program like Matlab or Maple, for example, it must be possible to find stability conditions on the coefficients of the system of ordinary differential equations from (4.9), and therefore find possible parameter values of g, τ, r, η, plus coupling $J(\mathbf{x})$, such that the stable pattern selected in the bifurcation at α^* is a travelling hexagonal activity pattern or a stationary, regularly oscillating hexagonal activity pattern.

Chapter 5

Conclusions

I have analyzed a model neuronal network introduced by Ermentrout and Curtu, extended to two space dimensions. The model can be seen as a simple model of a cortical sheet that describes the firing rate activity of two populations of neurons coupled together, one excitatory that displays linear adaptation and the other one inhibitory. The dynamics of the activity is described by a system of nonlocal partial integro-differential equations in which a nonlinear sigmoidal-shaped firing rate function is included. The synaptic coupling between the neurons is characterized by local excitation and long range inhibition. Running numerical simulations with the model shows that a stable travelling hexagonal activity pattern is a solution of the model given certain sets of values for the parameters of the model. I wanted to investigate the mechanism behind the formation of these patterns and the performed analysis have provided me with a clear picture of this mechanism.

The mathematical analysis shows that it is indeed possible for spatio-temporal patterns to start forming in the model when the uniform quiescent state loses stability in the bifurcation at α^*. The patterns start bifurcating from the uniform quiescent state when the gain of the adaptation is strong enough or the adaptation is slow enough which effectively results in a Hopf bifurcation. At this moment the stability of the trivial state is lost at pure imaginary pairs of eigenvalues belonging to the wave vectors of set $\mathbb{K}$ and the functions from the basis for the nullspace of the linear operator L_0 with wave vectors of set $\mathbb{K}$ form the basis for a center manifold. Based solely on the linear stability analysis it is expected that these solutions start growing without bounds. However, the nonlinear sigmoidal-shaped firing rate function prevents this and effectively limits this unbounded growth so that the patterns can form. The exact shape of the synaptic coupling function determines which wave vectors will be elements of set $\mathbb{K}$ and these elements determine the shapes of the patterns that can possibly form in the model. Which pattern stabilizes, if any, depends on the exact values of the parameters g, τ, r and η of the model. The values for these parameters determine the values of the coefficients of the system of ordinary differential equations which describes the evolution of the coefficients of a general solution which correspond to a certain type of activity pattern. The values for the parameters of the model determine the equilibrium solution(s) of the system of ordinary differential equations and their stability which in turn determines the type of pattern and the stability of the general solutions.

The spatio-temporal hexagonal patterns I have found as equilibrium solutions of the model consist of travelling hexagonal activity patterns and stationary, regularly oscillating hexagonal activity patterns. The former solution I have also found quite frequenctly as a stable solution in numerical simulations with the model. The latter solution, however, is a solution I've never found in numerical simulations and it is a new solution for me.

This makes it very unfortunate that I don't have the time anymore at present to determine the stability conditions on the coefficients of the system of ordinary differential equations from (4.9) for the found patterns, assuming that these conditions do exist. Provided with these conditions I would be able to find possible parameter values of g, τ, r, η, plus coupling $J(\mathbf{x})$ such that the stable pattern selected in the bifurcation at α^* is a stationary, regularly oscillating hexagonal activity pattern and this would allow me to demonstrate the pattern in numerical simulations with the model. Finding these conditions would furthermore provide me with a clear theorem about the conditions under which, which type of hexagonal activity pattern stabilizes as a solution of the model. But on the bright side, an algorithm has been presented and it is merely a matter of time to implement the algorithm and find the conditions.

The analysis also sheds some light on why I haven't found a semi-randomly translating hexagonal activity pattern as a stable solution of this type of model. The equilibrium solutions that I have found, are either hexagonal activity patterns with planar waves as constituting waves which travel over the plane with a constant velocity or (hexagonal) activity patterns with standing planar waves as constituting waves which are both periodic in space and time. These solutions are clearly different from a semi-randomly translating hexagonal activity pattern. I do not expect to find other equilibrium solutions in the model that correspond to spatio-temporal hexagonal activity patterns in the case of a Hopf bifurcation although I should mention that I haven't searched extensively for other solutions. I also cannot expect to find spatio-temporal hexagonal activity patterns in the case that the stability of the uniform quiescent state is lost at the moment one eigenvalue crosses the imaginary axis for each of the wave vectors of set $\mathbb{K}$. This scenario will lead to stationary hexagonal activity patterns.

This leaves me with one other option. Namely, the case when the stability of the uniform quiescent state is lost at pairs of zero eigenvalues. I do not expect to find the desired semi-randomly translating hexagonal activity pattern as a stable solution in this case, but I haven't investigated it either. Ermentrout and Curtu [6] mention the possibility of a stable modulated wave pattern in their model when the stability of the uniform quiescent state is lost at a pair of zero eigenvalues. This pattern bifurcates from a travelling wave solution through another Hopf bifurcation that introduces a new frequency in the solution and they describe this pattern as a pattern characterized by two different frequencies, one correspondig to the orbital motion and the other to radial oscillations. This sounds interesting and therefore I would like to study this double-zero bifurcation in model (2.1) to find out what type of (stable) activity patterns actually can be obtained in this case.

As a last note I also want to mention that the analysis of model (2.1) is not complete with respect to the overall shape of patterns that can form in the model. As mentioned above, the shape of the synaptic coupling function determines which wave vectors will be elements of set $\mathbb{K}$ and these elements determine the shapes of the patterns that can possibly form in the model. Playing around with the code of the numerical implementation of the model by choosing different combinations of values for the parameters of the model will result quite easily in stable solutions of the model which consist of patterns with a different overall shape. I have obtained, for example, stationary stripe and square activity patterns, stationary regularly oscillating square activity patterns and travelling square activity patterns. It might be interesting to determine under which conditions these and presumably other patterns will be stable and how they differ from and interact with the stability conditions of hexagonal activity patterns.

Appendix A

The singular perturbation analysis

I started by carrying out a proper scaling of the variables of the model and the bifurcation parameter with respect to the small perturbation quantity ϵ. Scaling solution $U(\mathbf{x}, t)$ results in

$$U(\mathbf{x}, t) = \epsilon U_0(\mathbf{x}, t) + \epsilon^2 U_1(\mathbf{x}, t) + \epsilon^3 U_2(\mathbf{x}, t) + \ldots = \epsilon \begin{pmatrix} u_0 \\ v_0 \end{pmatrix} + \epsilon^2 \begin{pmatrix} u_1 \\ v_1 \end{pmatrix} + \epsilon^3 \begin{pmatrix} u_2 \\ v_2 \end{pmatrix} + \ldots \tag{A.1}$$

A good scaling for the bifurcation parameter α is

$$\alpha = \alpha^* + \epsilon^2 \gamma \quad \text{with} \quad \epsilon \in \{\mathbb{R} \mid |\epsilon| \ll 1\}, \gamma \in \mathbb{R}. \tag{A.2}$$

The linearization of model (2.1) in linear and higher order terms (i.e. expansion (3.1)) can be written in the equivalent form

$$L_0 U = (\alpha - \alpha^*) \begin{pmatrix} J * u \\ 0 \end{pmatrix} + \begin{pmatrix} \frac{F''(0)}{2} (\alpha J * u - g v)^2 \\ 0 \end{pmatrix} + \begin{pmatrix} \frac{F'''(0)}{6} (\alpha J * u - g v)^3 \\ 0 \end{pmatrix} + \ldots \tag{A.3}$$

With the singular perturbation expansion (A.1), the first vector-component of equation (A.3) then reads as

$$\begin{aligned} [\epsilon L_0 U_0 + \epsilon^2 L_0 U_1 + \epsilon^3 L_0 U_2 + \mathcal{O}(\epsilon^4)]_{(1)} = \epsilon^2 \gamma J * u + \frac{F''(0)}{2} [\alpha^* J * u - g v + (\alpha - \alpha^*) J * u]^2 + \\ \frac{F'''(0)}{6} [\alpha^* J * u - g v + (\alpha - \alpha^*) J * u]^3 + \ldots = \epsilon^2 \frac{F''(0)}{2} [\alpha^* J * u_0 - g v_0]^2 + \\ \epsilon^3 \gamma (J * u_0) + \epsilon^3 F''(0) [\alpha^* J * u_0 - g v_0][\alpha^* J * u_1 - g v_1] + \epsilon^3 \frac{F'''(0)}{6} [\alpha^* J * u_0 - g v_0]^3 + \mathcal{O}(\epsilon^4), \end{aligned}$$

from which follows

$$\begin{aligned} [L_0 U_0 + \epsilon L_0 U_1 + \epsilon^2 L_0 U_2 + \mathcal{O}(\epsilon^3)]_{(1)} = \epsilon \frac{F''(0)}{2} [\alpha^* J * u_0 - g v_0]^2 + \epsilon^2 \{ \gamma (J * u_0 + \\ F''(0) [\alpha^* J * u_0 - g v_0][\alpha^* J * u_1 - g v_1] + \frac{F'''(0)}{6} [\alpha^* J * u_0 - g v_0]^3 \} + \mathcal{O}(\epsilon^3). \end{aligned} \tag{A.4}$$

The second vector-component of equation (A.3) reads as

$$[L_0 U_0 + \epsilon L_0 U_1 + \epsilon^2 L_0 U_0 + \mathcal{O}(\epsilon^3)]_{(2)} = 0. \tag{A.5}$$

The first equation that I needed to solve was $L_0 U_0 = \mathbf{0}$ which is exact up to the order $\mathcal{O}(\epsilon)$. In order to solve this equation I first considered the basis of the center manifold which has been determined in chapter 4. This basis consists of the following functions: $\{\boldsymbol{\Phi}_0 e^{i(\omega_0 t \pm \mathbf{k}_0^j \cdot \mathbf{x})}, \bar{\boldsymbol{\Phi}}_0 e^{-i(\omega_0 t \pm \mathbf{k}_0^j \cdot \mathbf{x})}\}$ for $\mathbf{k}_0^j \in \mathbb{K}$, $j = 1, 2, 3$ under the restriction that the angles between the different wave vectors are $2\pi/3$ radians with $\boldsymbol{\Phi}_0, \bar{\boldsymbol{\Phi}}_0$ and ω_0 defined by (4.2) and (4.3) respectively. Therefore the solution U_0 can be written as

$$U_0 = \sum_{j=1}^{3} \left(Z_j(\epsilon^2 t) \boldsymbol{\Phi}_0 e^{i(\omega_0 t + \mathbf{k}_0^j \cdot \mathbf{x})} + W_j(\epsilon^2 t) \boldsymbol{\Phi}_0 e^{i(\omega_0 t - \mathbf{k}_0^j \cdot \mathbf{x})} + c.c. \right), \tag{A.6}$$

where I have chosen the time scale $Z_j = Z_j(\epsilon^2 t)$ and $W_j = W_j(\epsilon^2 t)$ and with the abbreviation c.c. denoting the complex conjugation of the expression it follows within parentheses. Next I have expanded Z_j and W_j as

$$Z_j = Z_j(0) + Z_j'(0)\epsilon^2 t + \mathcal{O}(\epsilon^4) \quad \text{and} \quad W_j = W_j(0) + W_j'(0)\epsilon^2 t + \mathcal{O}(\epsilon^4). \tag{A.7}$$

Introducing (A.7) in (A.6) results in

$$\begin{aligned} U_0 = \sum_{j=1}^{3} \Big(\Big[Z_j(0) \boldsymbol{\Phi}_0 e^{i(\omega_0 t + \mathbf{k}_0^j \cdot \mathbf{x})} + W_j(0) \boldsymbol{\Phi}_0 e^{i(\omega_0 t - \mathbf{k}_0^j \cdot \mathbf{x})} + c.c. \Big] + \\ t\epsilon^2 \Big[Z_j'(0) \boldsymbol{\Phi}_0 e^{i(\omega_0 t + \mathbf{k}_0^j \cdot \mathbf{x})} + W_j'(0) \boldsymbol{\Phi}_0 e^{i(\omega_0 t - \mathbf{k}_0^j \cdot \mathbf{x})} + c.c. \Big] \Big) + \mathcal{O}(\epsilon^4). \end{aligned} \tag{A.8}$$

The following holds:

$$L_0(\boldsymbol{\Phi}_0 e^{i(\omega_0 t \pm \mathbf{k}_0^j \cdot \mathbf{x})}) = 0 \quad \text{and} \quad L_0(\bar{\boldsymbol{\Phi}}_0 e^{-i(\omega_0 t \pm \mathbf{k}_0^j \cdot \mathbf{x})}) = 0.$$

Therefore application of the linear operator L_0 on (A.8) results in

$$L_0 U_0 = \epsilon^2 \sum_{j=1}^{3} \left(Z_j'(0) L_0 \left(\boldsymbol{\Phi}_0 t e^{i(\omega_0 t + \mathbf{k}_0^j \cdot \mathbf{x})} \right) + W_j'(0) L_0 \left(\boldsymbol{\Phi}_0 t e^{i(\omega_0 t - \mathbf{k}_0^j \cdot \mathbf{x})} \right) + c.c. \right) + \mathcal{O}(\epsilon^4). \tag{A.9}$$

Application of the linear operator L_0 on $\boldsymbol{\Phi}_0 t e^{i(\omega_0 t \pm \mathbf{k}_0^j \cdot \mathbf{x})}$ gives

$$\frac{\partial}{\partial t} \left(\boldsymbol{\Phi}_0 t e^{i(\omega_0 t \pm \mathbf{k}_0^j \cdot \mathbf{x})} \right) - \begin{pmatrix} -1 + \alpha^* J * (\cdot) & -g \\ 1/\tau & -1/\tau \end{pmatrix} \boldsymbol{\Phi}_0 t e^{i(\omega_0 t \pm \mathbf{k}_0^j \cdot \mathbf{x})}.$$

This results in

$$\boldsymbol{\Phi}_0 e^{i(\omega_0 t \pm \mathbf{k}_0^j \cdot \mathbf{x})} + t \frac{\partial}{\partial t} \left(\boldsymbol{\Phi}_0 e^{i(\omega_0 t \pm \mathbf{k}_0^j \cdot \mathbf{x})} \right) - t \begin{pmatrix} -1 + \alpha^* J * (\cdot) & -g \\ 1/\tau & -1/\tau \end{pmatrix} \boldsymbol{\Phi}_0 e^{i(\omega_0 t \pm \mathbf{k}_0^j \cdot \mathbf{x})}.$$

This latter expression is equivalent with

$$\boldsymbol{\Phi}_0 e^{i(\omega_0 t \pm \mathbf{k}_0^j \cdot \mathbf{x})} + t L_0(\boldsymbol{\Phi}_0 e^{i(\omega_0 t \pm \mathbf{k}_0^j \cdot \mathbf{x})}).$$

The second term in the last expression is zero as was noted previously. Hence,

$$L_0 \left(\boldsymbol{\Phi}_0 t e^{i(\omega_0 t \pm \mathbf{k}_0^j \cdot \mathbf{x})} \right) = \boldsymbol{\Phi}_0 e^{i(\omega_0 t \pm \mathbf{k}_0^j \cdot \mathbf{x})}. \tag{A.10}$$

Along similar lines, I also obtained

$$L_0\left(\bar{\mathbf{\Phi}}_0 t e^{-i(\omega_0 t \pm \mathbf{k}_0^j \cdot \mathbf{x})}\right) = \bar{\mathbf{\Phi}}_0 e^{-i(\omega_0 t \pm \mathbf{k}_0^j \cdot \mathbf{x})}. \tag{A.11}$$

Introducing (A.10) and (A.11) in (A.9) results in the following expression for L_0U_0:

$$L_0U_0 = \epsilon^2 \sum_{j=1}^{3} \left(Z_j'(0)\left(\mathbf{\Phi}_0 e^{i(\omega_0 t + \mathbf{k}_0^j \cdot \mathbf{x})}\right) + W_j'(0)\left(\mathbf{\Phi}_0 e^{i(\omega_0 t - \mathbf{k}_0^j \cdot \mathbf{x})}\right) + c.c.\right) + \mathcal{O}(\epsilon^4). \tag{A.12}$$

The next equation that I needed to solve was $L_0U_1 = \frac{F''(0)}{2}\mathbf{S}$ with the first component of $\mathbf{S}$ defined by (A.17) while the second component of $\mathbf{S}$ is zero. This equation is also exact up to the order $\mathcal{O}(\epsilon)$ when using the solution U_0. I started by defining $D \in \mathbb{C}$ as

$$D := \left(1 + \frac{1}{\tau}, -g\right)\mathbf{\Phi}_0 = \phi + i\phi\frac{\sqrt{-1+g\tau}}{\tau} = \phi(1 + i\omega_0). \tag{A.13}$$

with $\mathbf{\Phi}_0$ and ω_0 defined respectively by (4.2) and (4.3). Subsequently I evaluated $J * u_0$ which resulted in

$$J * u_0 = \sum_{j=1}^{3} \left(\hat{J}(\mathbf{k}_0^j)\left[Z_j \mathbf{\Phi}_0^1 e^{i(\omega_0 t + \mathbf{k}_0^j \cdot \mathbf{x})} + W_j \mathbf{\Phi}_0^1 e^{i(\omega_0 t - \mathbf{k}_0^j \cdot \mathbf{x})} + c.c.\right]\right),$$

from which follows

$$J * u_0 = \sum_{j=1}^{3} \left(\hat{J}(\mathbf{k}_0^j)\left[\phi Z_j(0) e^{i(\omega_0 t + \mathbf{k}_0^j \cdot \mathbf{x})} + \phi W_j(0) e^{i(\omega_0 t - \mathbf{k}_0^j \cdot \mathbf{x})} + c.c.\right]\right) + \mathcal{O}(\epsilon^2). \tag{A.14}$$

In the latter equation I've made use of (A.7).

A similar evaluation of $\alpha^* J * u_0 - g v_0$ resulted in

$$\alpha^* J * u_0 - g v_0 = \sum_{j=1}^{3} \left(\left(1 + \frac{1}{\tau}\right) \left[Z_j(0) \mathbf{\Phi}_0^1 e^{i(\omega_0 t + \mathbf{k}_0^j \cdot \mathbf{x})} + W_j(0) \mathbf{\Phi}_0^1 e^{i(\omega_0 t - \mathbf{k}_0^j \cdot \mathbf{x})} + c.c. \right] - g \left[Z_j(0) \mathbf{\Phi}_0^2 e^{i(\omega_0 t + \mathbf{k}_0^j \cdot \mathbf{x})} + W_j(0) \mathbf{\Phi}_0^2 e^{i(\omega_0 t - \mathbf{k}_0^j \cdot \mathbf{x})} + c.c. \right] \right) + \mathcal{O}(\epsilon^2),$$

from which follows

$$\alpha^* J * u_0 - g v_0 = \sum_{j=1}^{3} \left(D \left[Z_j(0) e^{i(\omega_0 t + \mathbf{k}_0^j \cdot \mathbf{x})} + W_j(0) e^{i(\omega_0 t - \mathbf{k}_0^j \cdot \mathbf{x})} \right] + c.c. \right) + \mathcal{O}(\epsilon^2). \tag{A.15}$$

In the latter two equations I've made use of (A.7) and (A.13). Now, using equations (A.4), (A.12), (A.14) and (A.15) I obtained

$$L_0 U_1 = \frac{F''(0)}{2} \mathbf{S} + \epsilon \left[\mathbf{T} - \sum_{j=1}^{3} \left(Z_j'(0) \left(\mathbf{\Phi}_0 e^{i(\omega_0 t + \mathbf{k}_0^j \cdot \mathbf{x})} \right) + W_j'(0) \left(\mathbf{\Phi}_0 e^{i(\omega_0 t - \mathbf{k}_0^j \cdot \mathbf{x})} \right) + c.c. \right) - L_0 U_2 \right] + \mathcal{O}(\epsilon^2) \tag{A.16}$$

where the first vector-components of $\mathbf{S}$ and $\mathbf{T}$ are

$$\begin{aligned} \mathbf{S}_{(1)} = \sum_{j=1}^{3} \Bigg\{ \Bigg(D^2 \Bigg[& (Z_j(0))^2 e^{2i(\omega_0 t + \mathbf{k}_0^j \cdot \mathbf{x})} + (W_j(0))^2 e^{2i(\omega_0 t - \mathbf{k}_0^j \cdot \mathbf{x})} + \\ & Z_j(0) \sum_{\substack{l=1 \\ l \neq j}}^{3} \left(Z_l(0) e^{i(2\omega_0 t + (\mathbf{k}_0^j + \mathbf{k}_0^l) \cdot \mathbf{x})} \right) + W_j(0) \sum_{\substack{m=1 \\ m \neq j}}^{3} \left(W_m(0) e^{i(2\omega_0 t - (\mathbf{k}_0^j + \mathbf{k}_0^m) \cdot \mathbf{x})} \right) + \\ & 2 Z_j(0) \sum_{n=1}^{3} \left(W_n(0) e^{i(2\omega_0 t + (\mathbf{k}_0^j - \mathbf{k}_0^n) \cdot \mathbf{x})} \right) \Bigg] + D\bar{D} \Bigg[Z_j(0) \sum_{\substack{p=1 \\ p \neq j}}^{3} \left(\bar{Z}_p(0) e^{i((\mathbf{k}_0^j - \mathbf{k}_0^p) \cdot \mathbf{x})} \right) + \\ & W_j(0) \sum_{\substack{q=1 \\ q \neq j}}^{3} \left(\bar{W}_q(0) e^{i((\mathbf{k}_0^q - \mathbf{k}_0^j) \cdot \mathbf{x})} \right) + 2 Z_j(0) \sum_{r=1}^{3} \left(\bar{W}_r(0) e^{i((\mathbf{k}_0^j + \mathbf{k}_0^r) \cdot \mathbf{x})} \right) \Bigg] + \\ & c.c. \Bigg) + 2 D\bar{D} \Big[Z_j(0) \bar{Z}_j(0) + W_j(0) \bar{W}_j(0) \Big] \Bigg\} \end{aligned} \tag{A.17}$$

and

$$\mathbf{T}_{(1)} = \gamma \sum_{j=1}^{3} \left(\hat{J}(\mathbf{k}_0^j) \left[\phi Z_j(0) e^{i(\omega_0 t + \mathbf{k}_0^j \cdot \mathbf{x})} + \phi W_j(0) e^{i(\omega_0 t - \mathbf{k}_0^j \cdot \mathbf{x})} + c.c. \right] \right) +$$
$$F''(0) \sum_{j=1}^{3} \left(D \left[Z_j(0) e^{i(\omega_0 t + \mathbf{k}_0^j \cdot \mathbf{x})} + W_j(0) e^{i(\omega_0 t - \mathbf{k}_0^j \cdot \mathbf{x})} \right] + c.c. \right) [\alpha^* J * u_1 - g v_1] +$$
$$\frac{F'''(0)}{6} \left\{ \sum_{j=1}^{3} \left(D \left[Z_j(0) e^{i(\omega_0 t + \mathbf{k}_0^j \cdot \mathbf{x})} + W_j(0) e^{i(\omega_0 t - \mathbf{k}_0^j \cdot \mathbf{x})} \right] + c.c. \right) \right\}^3 \tag{A.18}$$

while the second vector-components are zero. Using the expanded form of $\mathbf{S}_{(1)}$ from (A.17) I could write U_1 in a similar manner, with $\xi_i \in \mathbb{C}^2$ for $i = \{\overline{1, 10}\}$, as

$$U_1 = \sum_{j=1}^{3} \Bigg\{ \Bigg(\xi_1^j (Z_j)^2 e^{2i(\omega_0 t + \mathbf{k}_0^j \cdot \mathbf{x})} + \xi_2^j (W_j)^2 e^{2i(\omega_0 t - \mathbf{k}_0^j \cdot \mathbf{x})} +$$
$$Z_j \sum_{\substack{l=1 \\ l \neq j}}^{3} \xi_3^{j,l} \left(Z_l e^{i(2\omega_0 t + (\mathbf{k}_0^j + \mathbf{k}_0^l) \cdot \mathbf{x})} \right) + W_j \sum_{\substack{m=1 \\ m \neq j}}^{3} \xi_4^{j,m} \left(W_m e^{i(2\omega_0 t - (\mathbf{k}_0^j + \mathbf{k}_0^m) \cdot \mathbf{x})} \right) +$$
$$Z_j \sum_{n=1}^{3} \xi_5^{j,n} \left(W_n e^{i(2\omega_0 t + (\mathbf{k}_0^j - \mathbf{k}_0^n) \cdot \mathbf{x})} \right) + Z_j \sum_{\substack{p=1 \\ p \neq j}}^{3} \xi_6^{j,p} \left(\bar{Z}_p e^{i((\mathbf{k}_0^j - \mathbf{k}_0^p) \cdot \mathbf{x})} \right) +$$
$$W_j \sum_{\substack{q=1 \\ q \neq j}}^{3} \xi_7^{j,q} \left(\bar{W}_q e^{i((\mathbf{k}_0^q - \mathbf{k}_0^j) \cdot \mathbf{x})} \right) + Z_j \sum_{r=1}^{3} \xi_8^{j,r} \left(\bar{W}_r e^{i((\mathbf{k}_0^j + \mathbf{k}_0^r) \cdot \mathbf{x})} \right) + c.c. \Bigg) +$$
$$\xi_9^j \left(Z_j \bar{Z}_j \right) + \xi_{10}^j \left(W_j \bar{W}_j \right) \Bigg\}.$$

Introducing (A.7) in the above equation results in

$$U_1 = \sum_{j=1}^{3} \Bigg\{ \Bigg(\xi_1^j (Z_j(0))^2 e^{2i(\omega_0 t + \mathbf{k}_0^j \cdot \mathbf{x})} + \xi_2^j (W_j(0))^2 e^{2i(\omega_0 t - \mathbf{k}_0^j \cdot \mathbf{x})} +$$
$$Z_j(0) \sum_{\substack{l=1 \\ l \neq j}}^{3} \xi_3^{j,l} \left(Z_l(0) e^{i(2\omega_0 t + (\mathbf{k}_0^j + \mathbf{k}_0^l) \cdot \mathbf{x})} \right) + W_j(0) \sum_{\substack{m=1 \\ m \neq j}}^{3} \xi_4^{j,m} \left(W_m(0) e^{i(2\omega_0 t - (\mathbf{k}_0^j + \mathbf{k}_0^m) \cdot \mathbf{x})} \right) +$$
$$Z_j(0) \sum_{n=1}^{3} \xi_5^{j,n} \left(W_n(0) e^{i(2\omega_0 t + (\mathbf{k}_0^j - \mathbf{k}_0^n) \cdot \mathbf{x})} \right) + Z_j(0) \sum_{\substack{p=1 \\ p \neq j}}^{3} \xi_6^{j,p} \left(\bar{Z}_p(0) e^{i((\mathbf{k}_0^j - \mathbf{k}_0^p) \cdot \mathbf{x})} \right) +$$
$$W_j(0) \sum_{\substack{q=1 \\ q \neq j}}^{3} \xi_7^{j,q} \left(\bar{W}_q(0) e^{i((\mathbf{k}_0^q - \mathbf{k}_0^j) \cdot \mathbf{x})} \right) + Z_j(0) \sum_{r=1}^{3} \xi_8^{j,r} \left(\bar{W}_r(0) e^{i((\mathbf{k}_0^j + \mathbf{k}_0^r) \cdot \mathbf{x})} \right) + c.c. \Bigg) +$$
$$\xi_9^j \left(Z_j(0) \bar{Z}_j(0) \right) + \xi_{10}^j \left(W_j(0) \bar{W}_j(0) \right) \Bigg\} + \mathcal{O}(\epsilon^2).$$

Application of the linear operator L_0 on the above equation results in

$$
\begin{aligned}
L_0U_1 = \sum_{j=1}^{3}\Bigg\{\Bigg(&\xi_1^j\left[2i\omega_0-\hat{L}(2\mathbf{k}_0^j)\right](Z_j(0))^2e^{2i(\omega_0t+\mathbf{k}_0^j\cdot\mathbf{x})}+\xi_2^j\left[2i\omega_0-\hat{L}(2\mathbf{k}_0^j)\right](W_j(0))^2e^{2i(\omega_0t-\mathbf{k}_0^j\cdot\mathbf{x})}+\\
&Z_j(0)\sum_{\substack{l=1\\l\neq j}}^{3}\xi_3^{j,l}\left[2i\omega_0-\hat{L}(\mathbf{k}_0^j+\mathbf{k}_0^l)\right]\left(Z_l(0)e^{i(2\omega_0t+(\mathbf{k}_0^j+\mathbf{k}_0^l)\cdot\mathbf{x})}\right)+\\
&W_j(0)\sum_{\substack{m=1\\m\neq j}}^{3}\xi_4^{j,m}\left[2i\omega_0-\hat{L}(\mathbf{k}_0^j+\mathbf{k}_0^m)\right]\left(W_m(0)e^{i(2\omega_0t-(\mathbf{k}_0^j+\mathbf{k}_0^m)\cdot\mathbf{x})}\right)+\\
&Z_j(0)\sum_{n=1}^{3}\xi_5^{j,n}\left[2i\omega_0-\hat{L}(\mathbf{k}_0^j-\mathbf{k}_0^n)\right]\left(W_n(0)e^{i(2\omega_0t+(\mathbf{k}_0^j-\mathbf{k}_0^n)\cdot\mathbf{x})}\right)-\\
&Z_j(0)\sum_{\substack{p=1\\p\neq j}}^{3}\xi_6^{j,p}\left[\hat{L}(\mathbf{k}_0^j-\mathbf{k}_0^p)\right]\left(\bar{Z}_p(0)e^{i((\mathbf{k}_0^j-\mathbf{k}_0^p)\cdot\mathbf{x})}\right)-\\
&W_j(0)\sum_{\substack{q=1\\q\neq j}}^{3}\xi_7^{j,q}\left[\hat{L}(\mathbf{k}_0^q-\mathbf{k}_0^j)\right]\left(\bar{W}_q(0)e^{i((\mathbf{k}_0^q-\mathbf{k}_0^j)\cdot\mathbf{x})}\right)-\\
&Z_j(0)\sum_{r=1}^{3}\xi_8^{j,r}\left[\hat{L}(\mathbf{k}_0^j+\mathbf{k}_0^r)\right]\left(\bar{W}_r(0)e^{i((\mathbf{k}_0^j+\mathbf{k}_0^r)\cdot\mathbf{x})}\right)+c.c.\Bigg)-\\
&\xi_9^j\hat{L}(\mathbf{0})\left(Z_j(0)\bar{Z}_j(0)\right)-\xi_{10}^j\hat{L}(\mathbf{0})\left(W_j(0)\bar{W}_j(0)\right)\Bigg\}+\mathcal{O}(\epsilon^2).
\end{aligned}
$$

Next I matched the coefficients of the terms $(Z_j(0))^2e^{2i(\omega_0t+\mathbf{k}_0^j\cdot\mathbf{x})}$, $(W_j(0))^2e^{2i(\omega_0t-\mathbf{k}_0^j\cdot\mathbf{x})}$, and so on in equation (A.16) with the coefficients in the above equation up to the order $\mathcal{O}(\epsilon)$. This results in

$$
\begin{aligned}
\xi_1^j=\xi_2^j&=\frac{D^2F''(0)}{2}\left[2i\omega_0\mathbf{I}-\hat{L}(2\mathbf{k}_0^j)\right]^{-1}\begin{pmatrix}1\\0\end{pmatrix}, & \xi_3^{j,l}&=\frac{D^2F''(0)}{2}\left[2i\omega_0\mathbf{I}-\hat{L}(\mathbf{k}_0^j+\mathbf{k}_0^l)\right]^{-1}\begin{pmatrix}1\\0\end{pmatrix},\\
\xi_4^{j,m}&=\frac{D^2F''(0)}{2}\left[2i\omega_0\mathbf{I}-\hat{L}(\mathbf{k}_0^j+\mathbf{k}_0^m)\right]^{-1}\begin{pmatrix}1\\0\end{pmatrix}, & \xi_5^{j,n}&=D^2F''(0)\left[2i\omega_0\mathbf{I}-\hat{L}(\mathbf{k}_0^j-\mathbf{k}_0^n)\right]^{-1}\begin{pmatrix}1\\0\end{pmatrix},\\
\xi_6^{j,p}&=\frac{-|D|^2F''(0)}{2}\left[\hat{L}(\mathbf{k}_0^j-\mathbf{k}_0^p)\right]^{-1}\begin{pmatrix}1\\0\end{pmatrix}, & \xi_7^{j,q}&=\frac{-|D|^2F''(0)}{2}\left[\hat{L}(\mathbf{k}_0^q-\mathbf{k}_0^j)\right]^{-1}\begin{pmatrix}1\\0\end{pmatrix},\\
\xi_8^{j,r}&=-|D|^2F''(0)\left[\hat{L}(\mathbf{k}_0^j+\mathbf{k}_0^r)\right]^{-1}\begin{pmatrix}1\\0\end{pmatrix}, & \xi_9^j=\xi_{10}^j&=-|D|^2F''(0)\left[\hat{L}(\mathbf{0})\right]^{-1}\begin{pmatrix}1\\0\end{pmatrix},
\end{aligned}
$$

or equivalently

$$\begin{aligned}
\xi_1^j = \xi_2^j &= \frac{D^2F''(0)}{2\left[\frac{3(1/\tau-g)}{\tau} + \left(\frac{1}{\tau}+2i\omega_0\right)\left(1+\frac{1}{\tau}\right)\left(1-\frac{\hat{J}(2\mathbf{k}_0^j)}{\hat{J}(\mathbf{k}_0^j)}\right)\right]}\begin{pmatrix}\frac{1}{\tau}+2i\omega_0\\ \frac{1}{\tau}\end{pmatrix},\\
\xi_3^{j,l} &= \frac{D^2F''(0)}{2\left[\frac{3(1/\tau-g)}{\tau} + \left(\frac{1}{\tau}+2i\omega_0\right)\left(1+\frac{1}{\tau}\right)\left(1-\frac{\hat{J}(\mathbf{k}_0^j+\mathbf{k}_0^l)}{\hat{J}(\mathbf{k}_0^j)}\right)\right]}\begin{pmatrix}\frac{1}{\tau}+2i\omega_0\\ \frac{1}{\tau}\end{pmatrix},\\
\xi_4^{j,m} &= \frac{D^2F''(0)}{2\left[\frac{3(1/\tau-g)}{\tau} + \left(\frac{1}{\tau}+2i\omega_0\right)\left(1+\frac{1}{\tau}\right)\left(1-\frac{\hat{J}(\mathbf{k}_0^j+\mathbf{k}_0^m)}{\hat{J}(\mathbf{k}_0^j)}\right)\right]}\begin{pmatrix}\frac{1}{\tau}+2i\omega_0\\ \frac{1}{\tau}\end{pmatrix},\\
\xi_5^{j,n} &= \frac{D^2F''(0)}{\frac{3(1/\tau-g)}{\tau} + \left(\frac{1}{\tau}+2i\omega_0\right)\left(1+\frac{1}{\tau}\right)\left(1-\frac{\hat{J}(\mathbf{k}_0^j-\mathbf{k}_0^n)}{\hat{J}(\mathbf{k}_0^j)}\right)}\begin{pmatrix}\frac{1}{\tau}+2i\omega_0\\ \frac{1}{\tau}\end{pmatrix},
\end{aligned}$$

$$\begin{aligned}
\xi_6^{j,p} &= \frac{|D|^2F''(0)}{2\left[g+1-\frac{(1+1/\tau)\hat{J}(\mathbf{k}_0^j-\mathbf{k}_0^p)}{\hat{J}(\mathbf{k}_0^j)}\right]}\begin{pmatrix}1\\1\end{pmatrix}, \quad \xi_7^{j,q} = \frac{|D|^2F''(0)}{2\left[g+1-\frac{(1+1/\tau)\hat{J}(\mathbf{k}_0^q-\mathbf{k}_0^j)}{\hat{J}(\mathbf{k}_0^j)}\right]}\begin{pmatrix}1\\1\end{pmatrix},\\
\xi_8^{j,r} &= \frac{|D|^2F''(0)}{g+1-\frac{(1+1/\tau)\hat{J}(\mathbf{k}_0^j+\mathbf{k}_0^r)}{\hat{J}(\mathbf{k}_0^j)}}\begin{pmatrix}1\\1\end{pmatrix}, \qquad \xi_9^j = \xi_{10}^j = \frac{|D|^2F''(0)}{g+1-\frac{(1+1/\tau)\hat{J}(\mathbf{0})}{\hat{J}(\mathbf{k}_0^j)}}\begin{pmatrix}1\\1\end{pmatrix}.
\end{aligned}$$

The last equation that I needed to solve was

$$L_0U_2 = \mathbf{T} - \sum_{j=1}^{3}\left(Z_j'(0)\left(\mathbf{\Phi}_0 e^{i(\omega_0 t+\mathbf{k}_0^j\cdot\mathbf{x})}\right) + W_j'(0)\left(\mathbf{\Phi}_0 e^{i(\omega_0 t-\mathbf{k}_0^j\cdot\mathbf{x})}\right) + c.c.\right) \tag{A.19}$$

which is also exact up to the order $\mathcal{O}(\epsilon)$ when using the solution U_0 and U_1 found above. This equation is a direct consequence of (A.16). I started by defining $K, L, M \in \mathbb{C}$ and $N, P, Q \in \mathbb{R}$ as

$$\begin{aligned}
\frac{D^2F''(0)}{2}K^j &:= \alpha^*\hat{J}(2\mathbf{k}_0^j)\xi_1^{j,1} - g\xi_1^{j,2} = \alpha^*\hat{J}(2\mathbf{k}_0^j)\xi_2^{j,1} - g\xi_2^{j,2},\\
\frac{D^2F''(0)}{2}L^{j,l} &:= \alpha^*\hat{J}(\mathbf{k}_0^j+\mathbf{k}_0^l)\xi_3^{j,l,1} - g\xi_3^{j,l,2} = \alpha^*\hat{J}(\mathbf{k}_0^j+\mathbf{k}_0^l)\xi_4^{j,l,1} - g\xi_4^{j,l,2},\\
D^2F''(0)M^{j,m} &:= \alpha^*\hat{J}(\mathbf{k}_0^j-\mathbf{k}_0^m)\xi_5^{j,m,1} - g\xi_5^{j,m,2},\\
\frac{|D|^2F''(0)}{2}N^{j,n} &:= \alpha^*\hat{J}(\mathbf{k}_0^j-\mathbf{k}_0^n)\xi_6^{j,n,1} - g\xi_6^{j,n,2} = \alpha^*\hat{J}(\mathbf{k}_0^n-\mathbf{k}_0^j)\xi_7^{j,n,1} - g\xi_7^{j,n,2},\\
|D|^2F''(0)P^{j,p} &:= \alpha^*\hat{J}(\mathbf{k}_0^j+\mathbf{k}_0^p)\xi_8^{j,p,1} - g\xi_8^{j,p,2},\\
|D|^2F''(0)Q^j &:= \alpha^*\hat{J}(\mathbf{0})\xi_9^{j,1} - g\xi_9^{j,2} = \alpha^*\hat{J}(\mathbf{0})\xi_{10}^{j,1} - g\xi_{10}^{j,2}.
\end{aligned}$$

Next I evaluated $\alpha^* J * u_1 - gv_1$ which resulted in

$$\alpha^* J * u_1 - gv_1 = \sum_{j=1}^{3} \Bigg\{ \Bigg(\frac{D^2 F''(0)}{2} K^j \left(Z_j(0)\right)^2 e^{2i(\omega_0 t + \mathbf{k}_0^j \cdot \mathbf{x})} + \frac{D^2 F''(0)}{2} K^j \left(W_j(0)\right)^2 e^{2i(\omega_0 t - \mathbf{k}_0^j \cdot \mathbf{x})} +$$

$$\frac{D^2 F''(0)}{2} Z_j(0) \sum_{\substack{l=1 \\ l \neq j}}^{3} L^{j,l} \left(Z_l(0) e^{i(2\omega_0 t + (\mathbf{k}_0^j + \mathbf{k}_0^l) \cdot \mathbf{x})} \right) + \frac{D^2 F''(0)}{2} W_j(0) \sum_{\substack{l=1 \\ l \neq j}}^{3} L^{j,l} \left(W_l(0) e^{i(2\omega_0 t - (\mathbf{k}_0^j + \mathbf{k}_0^l) \cdot \mathbf{x})} \right) +$$

$$D^2 F''(0) Z_j(0) \sum_{m=1}^{3} M^{j,m} \left(W_m(0) e^{i(2\omega_0 t + (\mathbf{k}_0^j - \mathbf{k}_0^m) \cdot \mathbf{x})} \right) + \frac{|D|^2 F''(0)}{2} Z_j(0) \sum_{\substack{n=1 \\ n \neq j}}^{3} N^{j,n} \left(\bar{Z}_n(0) e^{i((\mathbf{k}_0^j - \mathbf{k}_0^n) \cdot \mathbf{x})} \right) +$$

$$\frac{|D|^2 F''(0)}{2} W_j(0) \sum_{\substack{n=1 \\ n \neq j}}^{3} N^{j,n} \left(\bar{W}_n(0) e^{i((\mathbf{k}_0^n - \mathbf{k}_0^j) \cdot \mathbf{x})} \right) + |D|^2 F''(0) Z_j(0) \sum_{p=1}^{3} P^{j,p} \left(\bar{W}_p(0) e^{i((\mathbf{k}_0^j + \mathbf{k}_0^p) \cdot \mathbf{x})} \right) + c.c. \Bigg) +$$

$$|D|^2 F''(0) Q^j \left(Z_j(0) \bar{Z}_j(0) \right) + |D|^2 F''(0) Q^j \left(W_j(0) \bar{W}_j(0) \right) \Bigg\} + \mathcal{O}(\epsilon^2). \quad \text{(A.20)}$$

Subsequently I introduced the result from (A.20) into (A.18) and I determined the essential terms in $\mathbf{T}_{(1)}$. These terms are those that include the exponential $e^{i(\omega_0 t \pm \mathbf{k}_0^j \cdot \mathbf{x})}$ and their complex conjugates for $j = 1, 2, 3$. Therefore (A.18) also reads as

$$\begin{aligned}
\mathbf{T}_{(1)} = \sum_{j=1}^{3} \Bigg(\Bigg[& \gamma \hat{J}(\mathbf{k}_0^j) \phi Z_j(0) + (F''(0))^2 D|D|^2 \Bigg\{ Z_j(0)|Z_j(0)|^2 \left(\frac{K^j}{2} + Q^j \right) + Z_j(0)|W_j(0)|^2 Q^j + \\
& \sum_{l=1}^{3} \big(Z_j(0)|W_l(0)|^2 (M^{j,l} + P^{j,l}) \big) + \sum_{\substack{m=1 \\ m \neq j}}^{3} \big(Z_j(0)|Z_m(0)|^2 (L^{j,m} + N^{j,m}) \big) + \\
& \sum_{\substack{n=1 \\ n \neq j}}^{3} \big(Z_n(0) W_n(0) \bar{W}_j(0) (N^{j,n} + P^{j,n}) \big) \Bigg\} + \frac{F'''(0)}{6} D|D|^2 \Bigg\{ 3 Z_j(0)|Z_j(0)|^2 + \\
& 2 Z_j(0)|W_j(0)|^2 + 4 \sum_{l=1}^{3} \big(Z_j(0)|W_l(0)|^2 \big) + 4 \sum_{\substack{m=1 \\ m \neq j}}^{3} \big(Z_j(0)|Z_m(0)|^2 \big) + \\
& 4 \sum_{\substack{n=1 \\ n \neq j}}^{3} \big(Z_n(0) W_n(0) \bar{W}_j(0) \big) \Bigg\} \Bigg] e^{i(\omega_0 t + \mathbf{k}_0^j \cdot \mathbf{x})} + \\
\Bigg[& \gamma \hat{J}(\mathbf{k}_0^j) \phi W_j(0) + (F''(0))^2 D|D|^2 \Bigg\{ W_j(0)|W_j(0)|^2 \left(\frac{K^j}{2} + Q^j \right) + |Z_j(0)|^2 W_j(0) Q^j + \\
& \sum_{l=1}^{3} \big(|Z_l(0)|^2 W_j(0) (M^{j,l} + P^{j,l}) \big) + \sum_{\substack{m=1 \\ m \neq j}}^{3} \big(W_j(0)|W_m(0)|^2 (L^{j,m} + N^{j,m}) \big) + \\
& \sum_{\substack{n=1 \\ n \neq j}}^{3} \big(Z_n(0) \bar{Z}_j(0) W_n(0) (N^{j,n} + P^{j,n}) \big) \Bigg\} + \frac{F'''(0)}{6} D|D|^2 \Bigg\{ 3 W_j(0)|W_j(0)|^2 + \\
& 2 |Z_j(0)|^2 W_j(0) + 4 \sum_{l=1}^{3} \big(|Z_l(0)|^2 W_j(0) \big) + 4 \sum_{\substack{m=1 \\ m \neq j}}^{3} \big(W_j(0)|W_m(0)|^2 \big) + \\
& 4 \sum_{\substack{n=1 \\ n \neq j}}^{3} \big(Z_n(0) \bar{Z}_j(0) W_n(0) \big) \Bigg\} \Bigg] e^{i(\omega_0 t - \mathbf{k}_0^j \cdot \mathbf{x})} \Bigg) + c.c. + \ldots \qquad \text{(A.21)}
\end{aligned}$$

Now I was in the position to find a solution for (A.19). In order to have a solution I needed the right term of (A.19) to be orthogonal on the basis of the nullspace of the linear operator L_0^*, the adjoint operator of the linear operator L_0. Here I made use of the Fredholm alternative method [12]. I introduced the linear operator L_0^* in appendix B and subsequently I proved that this operator is indeed the adjoint operator of L_0 on the space of functions that satisfy the assumptions (4.4) (and in the case of a finite neuronal network also the assumptions (4.5)) with the (standard) inner product (B.4). The details of the proof are given in appendix B. I also provided the basis of the nullspace of L_0^* in appendix B which is (B.2). Therefore the following holds

$$< \mathbf{T} - \sum_{j=1}^{3} \left(Z_j'(0) \left(\mathbf{\Phi}_0 e^{i(\omega_0 t + \mathbf{k}_0^j \cdot \mathbf{x})} \right) + W_j'(0) \left(\mathbf{\Phi}_0 e^{i(\omega_0 t - \mathbf{k}_0^j \cdot \mathbf{x})} \right) + c.c. \right), \mathbf{\Psi}_0 e^{i(\omega_0 t \pm \mathbf{k}_0^j \cdot \mathbf{x})} >=$$

$$\int_0^{\frac{2\pi}{\omega_0}} \mathrm{d}\, t \iint_\Omega \left[\mathbf{T} - \sum_{j=1}^{3} \left(Z_j'(0) \left(\mathbf{\Phi}_0 e^{i(\omega_0 t + \mathbf{k}_0^j \cdot \mathbf{x})} \right) + W_j'(0) \left(\mathbf{\Phi}_0 e^{i(\omega_0 t - \mathbf{k}_0^j \cdot \mathbf{x})} \right) + c.c. \right) \right] \cdot \bar{\mathbf{\Psi}}_0 e^{-i(\omega_0 t \pm \mathbf{k}_0^j \cdot \mathbf{x})} \, \mathrm{d}\, \mathbf{x} = 0.$$

Based on the fact that $\mathbf{\Phi} \cdot \bar{\mathbf{\Psi}}_0 = 1$ and using $\mathbf{T}_{(1)}$ from (A.21) and $\mathbf{T}_{(2)} = 0$, I obtained

$$\begin{cases} Z_j'(0) = \tilde{a}^j Z_j(0) + b^j Z_j(0)|Z_j(0)|^2 + c^j Z_j(0)|W_j(0)|^2 + Z_j(0) \displaystyle\sum_{l=1}^{3} \left(d^{j,l} |W_l(0)|^2 \right) + \\ \qquad Z_j(0) \displaystyle\sum_{\substack{m=1 \\ m \neq j}}^{3} \left(e^{j,m} |Z_m(0)|^2 \right) + \bar{W}_j(0) \displaystyle\sum_{\substack{n=1 \\ n \neq j}}^{3} \left(f^{j,n} Z_n(0) W_n(0) \right), \\ W_j'(0) = \tilde{a}^j W_j(0) + b^j W_j(0)|W_j(0)|^2 + c^j W_j(0)|Z_j(0)|^2 + W_j(0) \displaystyle\sum_{l=1}^{3} \left(d^{j,l} |Z_l(0)|^2 \right) + \\ \qquad W_j(0) \displaystyle\sum_{\substack{m=1 \\ m \neq j}}^{3} \left(e^{j,m} |W_m(0)|^2 \right) + \bar{Z}_j(0) \displaystyle\sum_{\substack{n=1 \\ n \neq j}}^{3} \left(f^{j,n} Z_n(0) W_n(0) \right), \end{cases} \tag{A.22}$$

with

$$\begin{aligned} \tilde{a}^j &= \gamma \hat{J}(\mathbf{k}_0^j) \phi \bar{\mathbf{\Psi}}_0^1, \\ b^j &= |D|^2 D \bar{\mathbf{\Psi}}_0^1 \cdot \left[(F''(0))^2 \left(\frac{K^j}{2} + Q^j \right) + \frac{F'''(0)}{2} \right], \\ c^j &= |D|^2 D \bar{\mathbf{\Psi}}_0^1 \cdot \left[(F''(0))^2 Q^j + \frac{F'''(0)}{3} \right], \\ d^{j,l} &= |D|^2 D \bar{\mathbf{\Psi}}_0^1 \cdot \left[(F''(0))^2 \left(M^{j,l} + P^{j,l} \right) + \frac{2F'''(0)}{3} \right], \\ e^{j,m} &= |D|^2 D \bar{\mathbf{\Psi}}_0^1 \cdot \left[(F''(0))^2 \left(L^{j,m} + N^{j,m} \right) + \frac{2F'''(0)}{3} \right], \\ f^{j,n} &= |D|^2 D \bar{\mathbf{\Psi}}_0^1 \cdot \left[(F''(0))^2 \left(N^{j,n} + P^{j,n} \right) + \frac{2F'''(0)}{3} \right]. \end{aligned} \tag{A.23}$$

The time variable in the above is $\epsilon^2 t$, $\tilde{a}^j = a^j/\epsilon^2$ and $a^j, b^j, c^j, d^{j,l}, e^{j,m}, f^{j,n}$ are of order 1. After applying the scaling $\epsilon Z_j(0) \leftrightarrow Z_j, \epsilon W_j(0) \leftrightarrow W_j$, and $\epsilon^2 t \leftrightarrow t$, I obtained

$$\begin{cases} Z_j'(t) = a^j Z_j(t) + b^j Z_j(t)|Z_j(t)|^2 + c^j Z_j(t)|W_j(t)|^2 + Z_j(t) \displaystyle\sum_{l=1}^{3} \left(d^{j,l} |W_l(t)|^2 \right) + \\ \qquad Z_j(t) \displaystyle\sum_{\substack{m=1 \\ m \neq j}}^{3} \left(e^{j,m} |Z_m(t)|^2 \right) + \bar{W}_j(t) \displaystyle\sum_{\substack{n=1 \\ n \neq j}}^{3} \left(f^{j,n} Z_n(t) W_n(t) \right), \\ W_j'(t) = a^j W_j(t) + b^j W_j(t)|W_j(t)|^2 + c^j W_j(t)|Z_j(t)|^2 + W_j(t) \displaystyle\sum_{l=1}^{3} \left(d^{j,l} |Z_l(t)|^2 \right) + \\ \qquad W_j(t) \displaystyle\sum_{\substack{m=1 \\ m \neq j}}^{3} \left(e^{j,m} |W_m(t)|^2 \right) + \bar{Z}_j(t) \displaystyle\sum_{\substack{n=1 \\ n \neq j}}^{3} \left(f^{j,n} Z_n(t) W_n(t) \right), \end{cases} \tag{A.24}$$

for $j = 1, 2, 3$. Hence, the sought-after general solution can be approximated by

$$\begin{aligned} U(\mathbf{x}, t) \approx 2\mathrm{Re} \Big\{ \mathbf{\Phi}_0 \Big[& Z_1(t) e^{i(\omega_0 t + \mathbf{k}_0^1 \cdot \mathbf{x})} + Z_2(t) e^{i(\omega_0 t + \mathbf{k}_0^2 \cdot \mathbf{x})} + Z_3(t) e^{i(\omega_0 t + \mathbf{k}_0^3 \cdot \mathbf{x})} + \\ & W_1(t) e^{i(\omega_0 t - \mathbf{k}_0^1 \cdot \mathbf{x})} + W_2(t) e^{i(\omega_0 t - \mathbf{k}_0^2 \cdot \mathbf{x})} + W_3(t) e^{i(\omega_0 t - \mathbf{k}_0^3 \cdot \mathbf{x})} \Big] \Big\} \end{aligned} \tag{A.25}$$

with $\mathbf{k}_0^j \in \mathbb{K}$ for $j = 1, 2, 3$ under the restriction that the angles between the different wave vectors are $2\pi/3$ radians. The coefficients $Z_j(t), W_j(t)$ for $j = 1, 2, 3$ satisfy the system of ordinary differential equations defined above.

As a final step I have rewritten the coefficients of this system of ordinary differential equations in order to help me find equilibrium solutions of this system in chapter 4. Equations (4.3), (B.3) and (A.13) imply

$$\begin{aligned}
\phi\bar{\mathbf{\Psi}}_0^1 &= \frac{1}{2} - i\frac{1}{2\sqrt{g\tau - 1}}, \\
D\bar{\mathbf{\Psi}}_0^1 &= \frac{1 + 1/\tau}{2} + i\frac{g - (1 + 1/\tau}{2\sqrt{g\tau - 1}}.
\end{aligned}$$

Therefore I could write $a^j, b^j, c^j, d^{j,l}, e^{j,m}, f^{j,n}$, using $\gamma = (\alpha - \alpha^*)/\epsilon^2$, $\alpha^* \hat{J}(\mathbf{k}_0^j) = 1 + 1/\tau$ and $\tilde{a}^j = a^j/\epsilon^2$, as

$$\begin{aligned}
a^j &= a_1^j + ia_2^j, & b^j &= b_1^j + ib_2^j, \\
c^j &= c_1^j + ic_2^j, & d^{j,l} &= d_1^{j,l} + id_2^{j,l}, \\
e^{j,m} &= e_1^{j,m} + ie_2^{j,m}, & f^{j,n} &= f_1^{j,n} + if_2^{j,n},
\end{aligned}$$

with

$$a_1^j = \frac{\alpha\hat{J}(\mathbf{k}_0^j) - (1 + 1/\tau)}{2}, \quad a_2^j = -\frac{\alpha\hat{J}(\mathbf{k}_0^j) - (1 + 1/\tau)}{2\sqrt{g\tau - 1}},$$

$$b_1^j = \frac{\tau + 1}{4\tau}|D|^2 \left[(F''(0))^2 \left(\mathrm{Re}(K^j) + \frac{1 - g\tau/(\tau + 1)}{\sqrt{g\tau - 1}} \mathrm{Im}(K^j) + 2Q^j \right) + F'''(0) \right],$$

$$b_2^j = \frac{g\tau - (\tau + 1)}{4\tau\sqrt{g\tau - 1}}|D|^2 \left[(F''(0))^2 \left(\mathrm{Re}(K^j) - \frac{1 - g\tau/(\tau + 1)}{\sqrt{g\tau - 1}} \mathrm{Im}(K^j) + 2Q^j \right) + F'''(0) \right],$$

$$c_1^j = \frac{\tau + 1}{4\tau}|D|^2 \left[2(F''(0))^2 Q^j + \frac{2F'''(0)}{3} \right],$$

$$c_2^j = \frac{g\tau - (\tau + 1)}{4\tau\sqrt{g\tau - 1}}|D|^2 \left[2(F''(0))^2 Q^j + \frac{2F'''(0)}{3} \right],$$

$$d_1^{j,l} = \frac{\tau + 1}{4\tau}|D|^2 \left[(F''(0))^2 \left(2\mathrm{Re}(M^{j,l}) + 2\frac{1 - g\tau/(\tau + 1)}{\sqrt{g\tau - 1}} \mathrm{Im}(M^{j,l}) + 2P^{j,l} \right) + \frac{4F'''(0)}{3} \right],$$

$$d_2^{j,l} = \frac{g\tau - (\tau + 1)}{4\tau\sqrt{g\tau - 1}}|D|^2 \left[(F''(0))^2 \left(2\mathrm{Re}(M^{j,l}) - 2\frac{1 - g\tau/(\tau + 1)}{\sqrt{g\tau - 1}} \mathrm{Im}(M^{j,l}) + 2P^{j,l} \right) + \frac{4F'''(0)}{3} \right],$$

$$e_1^{j,m} = \frac{\tau + 1}{4\tau}|D|^2 \left[(F''(0))^2 \left(2\mathrm{Re}(L^{j,m}) + 2\frac{1 - g\tau/(\tau + 1)}{\sqrt{g\tau - 1}} \mathrm{Im}(L^{j,m}) + 2N^{j,m} \right) + \frac{4F'''(0)}{3} \right],$$

$$e_2^{j,m} = \frac{g\tau - (\tau + 1)}{4\tau\sqrt{g\tau - 1}}|D|^2 \left[(F''(0))^2 \left(2\mathrm{Re}(L^{j,m}) - 2\frac{1 - g\tau/(\tau + 1)}{\sqrt{g\tau - 1}} \mathrm{Im}(L^{j,m}) + 2P^{j,m} \right) + \frac{4F'''(0)}{3} \right],$$

$$f_1^{j,n} = \frac{\tau + 1}{4\tau}|D|^2 \left[2(F''(0))^2 \left(N^{j,n} + P^{j,n} \right) + \frac{4F'''(0)}{3} \right],$$

$$f_2^{j,n} = \frac{g\tau - (\tau + 1)}{4\tau\sqrt{g\tau - 1}}|D|^2 \left[2(F''(0))^2 \left(N^{j,n} + P^{j,n} \right) + \frac{4F'''(0)}{3} \right]. \tag{A.26}$$

Appendix B

L_0^*, the adjoint operator of L_0

I introduce the following linear operator

$$L_0^* = -\frac{\partial}{\partial t} - \begin{pmatrix} -1 + \alpha J * (\cdot) & 1/\tau \\ -g & -1/\tau \end{pmatrix}. \tag{B.1}$$

It should be noted that both the linear operator L_0^* defined above, and the associated linear evolution matrix defined for all $\mathbf{k}_0^j \in \mathbb{K}$ (i.e. the matrix $\hat{L}(\mathbf{k}_0^j)^{\mathrm{T}}$), have been evaluated at $\alpha = \alpha^*$ while the value of the parameters τ and g were fixed in such a way that bifurcation condition (4.1) is met. A linear stability analysis of L_0^* followed up by a reasoning along similar lines to the reasoning in chapter 4 of this report shows that the operator that corresponds to the restriction of L_0^* on the space of functions that satisfy (4.4) (and in the case of a finite neuronal network also the assumptions (4.5)) has a twelve-dimensional nullspace with the basis

$$\mathbf{\Psi}_0 e^{i(\omega_0 t \pm \mathbf{k}_0^j \cdot \mathbf{x})} \quad \text{and} \quad \bar{\mathbf{\Psi}}_0 e^{-i(\omega_0 t \pm \mathbf{k}_0^j \cdot \mathbf{x})} \quad \text{with} \quad \mathbf{k}_0^j \in \mathbb{K} \tag{B.2}$$

for $j = 1, 2, 3$, under the restriction that the angles between the different wave vectors are $2\pi/3$ radians with ω_0 as defined by (4.2). The vectors $\mathbf{\Psi}_0$ and $\bar{\mathbf{\Psi}}_0$ are the two-dimensional complex eigenvectors of matrix $\hat{L}(\mathbf{k}_0^j)^{\mathrm{T}}$ and satisfy

$$\hat{L}(\mathbf{k}_0^j)^{\mathrm{T}} \mathbf{\Psi}_0 = -i\omega_0 \mathbf{\Psi}_0, \quad \hat{L}(\mathbf{k}_0^j)^{\mathrm{T}} \bar{\mathbf{\Psi}}_0 = i\omega_0 \bar{\mathbf{\Psi}}_0 \quad \text{and} \quad \mathbf{\Phi}_0 \cdot \bar{\mathbf{\Psi}}_0 = 1 \tag{B.3}$$

with the latter property introduced to simplify calculations. In order to be able to use the basis for the nullspace of the linear operator L_0^* in the Fredholm alternative method, I had to show that the linear operator L_0^* is the adjoint operator of L_0 on the space of functions that satisfy the assumptions (4.4) (and in the case of a finite neuronal network also the assumptions (4.5)) with the (standard) inner product

$$< N, M >= \int_0^{\frac{2\pi}{\omega_0}} \mathrm{d}\, t \iint_\Omega N(\mathbf{x}, t) \bar{M}(\mathbf{x}, t) \, \mathrm{d}\, \mathbf{x} = \int_0^{\frac{2\pi}{\omega_0}} \mathrm{d}\, t \iint_\Omega \left[n_1(\mathbf{x}, t) \bar{m}_1(\mathbf{x}, t) + n_2(\mathbf{x}, t) \bar{m}_2(\mathbf{x}, t) \right] \mathrm{d}\, \mathbf{x}. \tag{B.4}$$

In order to prove that L_0^* is the adjoint operator of L_0, I have considered two functions $N(\mathbf{x}, t)$ and $M(\mathbf{x}, t)$ that satisfy the assumptions (4.4) (and in the case of a finite neuronal network also the assumptions (4.5)) and I have computed (using the periodicity of n_j and m_j for $j = 1, 2$ with respect to t)

$$< N, L_0 M > - < L_0^* N, M > = \int_0^{\frac{2\pi}{\omega_0}} \mathrm{d}\, t \iint_\Omega \left[n_1 \frac{\mathrm{d}\, \bar{m}_1}{\mathrm{d}\, t} + \bar{m}_1 \frac{\mathrm{d}\, n_1}{\mathrm{d}\, t} + n_2 \frac{\mathrm{d}\, \bar{m}_2}{\mathrm{d}\, t} + \right.$$
$$\left. \bar{m}_2 \frac{\mathrm{d}\, n_2}{\mathrm{d}\, t} - \alpha^* n_1 (J * \bar{m}_1) + \alpha^* \bar{m}_1 (J * n_1) \right] \mathrm{d}\, \mathbf{x}.$$

Using integration by parts and the periodicity of the integrands with respect to t once more, the above equation reduces to

$$< N, L_0 M > - < L_0^* N, M > = \alpha^* \int_0^{\frac{2\pi}{\omega_0}} \mathrm{d}\, t \iint_\Omega \left[\bar{m}_1 (J * n_1) - n_1 (J * \bar{m}_1) \right] \mathrm{d}\, \mathbf{x}.$$

Next I needed to show that the inner double integral is zero for any fixed t, because then the righthand-side of the above equation vanishes. This would imply $< N, L_0 M > = < L_0^* N, M >$ for all functions N, M in the space of functions that satisfy the assumptions (4.4) (and in the case of a finite neuronal network also the assumptions (4.5)) by which I would have proven that L_0^* is the adjoint operator of L_0. Hence, I needed to prove that the following equation holds true:

$$\iint_\Omega \left[\bar{m}_1 (J * n_1) - n_1 (J * \bar{m}_1) \right] \mathrm{d}\, \mathbf{x} = 0 \tag{B.5}$$

on the space of complex functions at least $\mathcal{C}^2$ and such that

$$n(x, y) = n \left(x + \cos(\beta + \varphi) \frac{2\pi}{k_0}, y + \sin(\beta + \varphi) \frac{2\pi}{k_0} \right)$$

for all $x, y \in \Omega$ with $\Omega = [-l, l] \times [-l, l]$ where $l \in \{\mathbb{R}_{>0}, \infty\}$, $\beta \in [0, \pi/3\rangle$, random, but fixed and $\varphi \in \{r\pi/3 \mid r = \{0, 1, 2, 3, 4, 5\}\}$. k_0 is defined by (3.7). In the case of a finite neuronal network (i.e. $l \in \mathbb{R}_{>0}$) these functions must furthermore satisfy

$$n(-l, -l < y < l) = n(l, -l < y < l) \quad \text{and} \quad n(-l < x < l, -l) = n(-l < x < l, l).$$

The associated (standard) inner product with this space is defined as

$$< n, m > = \iint_\Omega n(\mathbf{x}) \bar{m}(\mathbf{x}) \, \mathrm{d}\, \mathbf{x}.$$

I furthermore defined on this space the operator $J * n(x, y)$ which represents the double convolution given by

$$(J * n)(x, y) = \iint_\Omega J(x - v, y - w) n(v, w) \, \mathrm{d}\, v \, \mathrm{d}\, w.$$

Herein represents the function $J(x, y)$ the function defined by (2.3). In order to prove (B.5), the first step that needed to be taken was to prove that $J * n(x, y)$ also satisfies

$$(J * n)(x, y) = (J * n) \left(x + \cos(\theta + \varphi) \frac{2\pi}{k_0}, y + \sin(\theta + \varphi) \frac{2\pi}{k_0} \right)$$

so that the inner products $< n, J * m >$ and $< J * n, m >$ make sense. In the case of an infinite neuronal network (i.e. $l = \infty$), the equality followes when considering changes of variables and the periodicity of the function $n(x, y)$:

$$\begin{aligned}
(J * n)\left(x + \cos(\theta+\varphi)\frac{2\pi}{k_0}, y + \sin(\theta+\varphi)\frac{2\pi}{k_0}\right) &= \\
\int_{-\infty}^{\infty}\int_{-\infty}^{\infty} J\left(x + \cos(\theta+\varphi)\frac{2\pi}{k_0} - v, y + \sin(\theta+\varphi)\frac{2\pi}{k_0} - w\right) n(v, w)\,\mathrm{d}\,v\,\mathrm{d}\,w &= \\
\int_{-\infty}^{\infty}\int_{-\infty}^{\infty} J\left(x - v, y - w\right) n\left(v + \cos(\theta+\varphi)\frac{2\pi}{k_0}, w + \sin(\theta+\varphi)\frac{2\pi}{k_0}\right)\mathrm{d}\,v\,\mathrm{d}\,w &= \\
\int_{-\infty}^{\infty}\int_{-\infty}^{\infty} J(x - v, y - w) n(v, w)\,\mathrm{d}\,v\,\mathrm{d}\,w &= (J * n)(x, y).
\end{aligned}$$

In the case of a finite neuronal network (i.e. $l \in \mathbb{R}_{>0}$), the equality is a consequence of the following derivation:

$$\begin{aligned}
(J * n)\left(x + \cos(\theta+\varphi)\frac{2\pi}{k_0}, y + \sin(\theta+\varphi)\frac{2\pi}{k_0}\right) &= \\
\int_{-l}^{l}\int_{-l}^{l} J\left(x + \cos(\theta+\varphi)\frac{2\pi}{k_0} - v, y + \sin(\theta+\varphi)\frac{2\pi}{k_0} - w\right) n(v, w)\,\mathrm{d}\,v\,\mathrm{d}\,w &= \\
\int_{-l-a}^{l-a}\int_{-l-b}^{l-b} J\left(x - v, y - w\right) n\left(v + \cos(\theta+\varphi)\frac{2\pi}{k_0}, w + \sin(\theta+\varphi)\frac{2\pi}{k_0}\right)\mathrm{d}\,v\,\mathrm{d}\,w &= \\
\int_{-l-a}^{l-a}\int_{-l-b}^{l-b} J\left(x - v, y - w\right) n\left(v, w\right)\mathrm{d}\,v\,\mathrm{d}\,w &= \\
\int_{-l}^{l}\int_{-l}^{l} J(x - v, y - w) n(v, w)\,\mathrm{d}\,v\,\mathrm{d}\,w &= (J * n)(x, y)
\end{aligned}$$

with $a = \cos(\theta+\varphi)(2\pi)/k_0$ and $b = \sin(\theta+\varphi)(2\pi)/k_0$. The second to last equality in the above derivation is a direct consequence of the double periodicity of both function J and function $n(x, y)$.

Now I needed to prove $< n, J * m >=< J * n, m >$, i.e.

$$\iint_{\Omega} n(\mathbf{x})(J * \bar{m}(\mathbf{x}))\,\mathrm{d}\,\mathbf{x} = \iint_{\Omega} (J * n(\mathbf{x}))\bar{m}(\mathbf{x})\,\mathrm{d}\,\mathbf{x}.$$

In order to accomplish this, I considered the Fourier transform of the functions $n(\mathbf{x})$ and $m(\mathbf{x})$, i.e.

$$n(\mathbf{x}) = \frac{1}{4l^2}\sum_{\mathbf{q}\in\mathbb{Z}^2} \hat{c}(\mathbf{q}) e^{\frac{i\pi(\mathbf{q}\cdot\mathbf{x})}{l}} \quad \text{and} \quad m(\mathbf{x}) = \frac{1}{4l^2}\sum_{\mathbf{r}\in\mathbb{Z}^2} \hat{d}(\mathbf{r}) e^{\frac{i\pi(\mathbf{r}\cdot\mathbf{x})}{l}}$$

in the case of a finite neuronal network and

$$n(\mathbf{x}) = \frac{1}{4\pi^2} \int_{-\infty}^{\infty} \int_{-\infty}^{\infty} \hat{c}(\mathbf{q}) e^{\frac{i\pi(\mathbf{q}\cdot\mathbf{x})}{l}} \,\mathrm{d}\,\mathbf{q} \quad \text{and} \quad m(\mathbf{x}) = \frac{1}{4\pi^2} \int_{-\infty}^{\infty} \int_{-\infty}^{\infty} \hat{d}(\mathbf{r}) e^{\frac{i\pi(\mathbf{r}\cdot\mathbf{x})}{l}} \,\mathrm{d}\,\mathbf{r}$$

in the case of an infinite neuronal network with the coefficients in both cases equal to

$$\hat{c}(\mathbf{q}) = \iint_{\Omega} n(\mathbf{p}) e^{\frac{-i\pi(\mathbf{p}\cdot\mathbf{q})}{l}} \,\mathrm{d}\,\mathbf{p} \quad \text{and} \quad \hat{d}(\mathbf{r}) = \iint_{\Omega} m(\mathbf{p}) e^{\frac{-i\pi(\mathbf{p}\cdot\mathbf{r})}{l}} \,\mathrm{d}\,\mathbf{p}.$$

Since I assumed $n, m \in \mathcal{C}^2$, their attached Fourier series converge uniformly on each closed interval in $\mathbb{R}^2$ (See for example the textbook of Loukas Grafakos [8] on this subject) and they sum up to n and m respectively. Moreover the coefficients of the Fourier series satisfy the condition

$$|\hat{c}(\mathbf{q})| = \mathcal{O}\left(\frac{1}{|\mathbf{q}|^2}\right), \quad |\hat{d}(\mathbf{r})| = \mathcal{O}\left(\frac{1}{|\mathbf{r}|^2}\right), \quad \text{as} \quad |\mathbf{q}|, |\mathbf{r}| \to \infty. \tag{B.6}$$

In the case of an infinite neuronal network, I have for any fixed $\mathbf{x} \in \mathbb{R}^2$,

$$J{*}n(\mathbf{x}) = \frac{1}{4\pi^2} \iint_{\Omega} J(\mathbf{x}{-}\mathbf{v}) \int_{-\infty}^{\infty} \int_{-\infty}^{\infty} \hat{c}(\mathbf{q}) e^{\frac{i\pi(\mathbf{q}\cdot\mathbf{v})}{l}} \,\mathrm{d}\,\mathbf{q}\,\mathrm{d}\,\mathbf{v} = \frac{1}{4\pi^2} \iint_{\Omega} J(\mathbf{x}{-}\mathbf{v}) \lim_{R\to\infty} \int_{-R}^{R} \int_{-R}^{R} \hat{c}(\mathbf{q}) e^{\frac{i\pi(\mathbf{q}\cdot\mathbf{v})}{l}} \,\mathrm{d}\,\mathbf{q}\,\mathrm{d}\,\mathbf{v} =$$

$$\frac{1}{4\pi^2} \iint_{\Omega} \lim_{R\to\infty} \left(\int_{-R}^{R} \int_{-R}^{R} \hat{c}(\mathbf{q}) J(\mathbf{x}-\mathbf{v}) e^{\frac{i\pi(\mathbf{q}\cdot\mathbf{v})}{l}} \,\mathrm{d}\,\mathbf{q} \right) \mathrm{d}\,\mathbf{v} = \frac{1}{4\pi^2} \iint_{\Omega} \lim_{R\to\infty} f_R(\mathbf{v}) \,\mathrm{d}\,\mathbf{v}.$$

I have $\lim_{R\to\infty} f_R(\mathbf{v}) = J(\mathbf{x}-\mathbf{v})n(\mathbf{v})$ for any $\mathbf{v} \in \mathbb{R}^2$, and based on conditions (B.6) there exists a function g such that $|f_R(\mathbf{v}| \leq g(\mathbf{v})$ for any R and $\mathbf{v} \in \mathbb{R}^2$ with $\iint_\Omega g(\mathbf{v}) \,\mathrm{d}\,\mathbf{v} < \infty$. Therefore I could apply Lebesgue's dominated convergence theorem [1] and I have obtained

$$J * n(\mathbf{x}) = \lim_{R\to\infty} \left(\frac{1}{4\pi^2} \int_{-R}^{R} \int_{-R}^{R} \hat{c}(\mathbf{q}) e^{\frac{i\pi(\mathbf{q}\cdot\mathbf{x})}{l}} \iint_{\Omega} J(\mathbf{x}-\mathbf{v}) e^{\frac{i\pi(\mathbf{q}\cdot(\mathbf{v}-\mathbf{x}))}{l}} \,\mathrm{d}\,\mathbf{v}\,\mathrm{d}\,\mathbf{q} \right) =$$

$$\frac{1}{4\pi^2} \int_{-\infty}^{\infty} \int_{-\infty}^{\infty} \hat{J}\left(\frac{\pi\mathbf{q}}{l}\right) \hat{c}(\mathbf{q}) e^{\frac{i\pi(\mathbf{q}\cdot\mathbf{x})}{l}} \,\mathrm{d}\,\mathbf{q}.$$

In a similar manner I have obtained

$$J * \bar{m}(\mathbf{x}) = \frac{1}{4\pi^2} \int_{-\infty}^{\infty} \int_{-\infty}^{\infty} \hat{J}\left(\frac{\pi\mathbf{r}}{l}\right) \bar{\hat{d}}(\mathbf{r}) e^{\frac{i\pi(\mathbf{r}\cdot\mathbf{x})}{l}} \,\mathrm{d}\,\mathbf{r}.$$

This implies

$$< J * n, m >= \iint_{\Omega} (J * n(\mathbf{x})) \bar{m}(\mathbf{x}) \,\mathrm{d}\,\mathbf{x} =$$

$$\frac{1}{16\pi^4} \int_{-\infty}^{\infty} \int_{-\infty}^{\infty} \int_{-\infty}^{\infty} \int_{-\infty}^{\infty} \hat{c}(\mathbf{q}) \hat{J}\left(\frac{\pi\mathbf{q}}{l}\right) \bar{\hat{d}}(\mathbf{r}) \iint_{\Omega} e^{\frac{i\pi(\mathbf{q}\cdot\mathbf{x})}{l}} e^{\frac{-i\pi(\mathbf{r}\cdot\mathbf{x})}{l}} \,\mathrm{d}\,\mathbf{x}\,\mathrm{d}\,\mathbf{q}\,\mathrm{d}\,\mathbf{r}$$

and

$$< n, J * m >= \iint\limits_{\Omega} n(\mathbf{x})(J * \bar{m}(\mathbf{x}))\,\mathrm{d}\,\mathbf{x} =$$
$$\frac{1}{16\pi^4} \int\limits_{-\infty}^{\infty}\int\limits_{-\infty}^{\infty}\int\limits_{-\infty}^{\infty}\int\limits_{-\infty}^{\infty} \hat{c}(\mathbf{q})\bar{\hat{d}}(\mathbf{r})\hat{J}\left(\frac{\pi\mathbf{r}}{l}\right)\iint\limits_{\Omega} e^{\frac{i\pi(\mathbf{q}\cdot\mathbf{x})}{l}} e^{\frac{-i\pi(\mathbf{r}\cdot\mathbf{x})}{l}}\,\mathrm{d}\,\mathbf{x}\,\mathrm{d}\,\mathbf{r}\,\mathrm{d}\,\mathbf{q}$$

and concludes the proof of $< n, J * m >=< J * n, m >$ in the case of an infinite neuronal network. It implies that equation (B.5) holds and in turn implies that the linear operator L_0^* is indeed the adjoint operator of the linear operator L_0 for infinite neuronal networks.

In the case of a finite neuronal network, I have, for any fixed $\mathbf{x} \in \mathbb{R}^2$ and $R \in \mathbb{Z}^2$,

$$J * n(\mathbf{x}) = \frac{1}{4l^2}\iint\limits_{\Omega} J(\mathbf{x}-\mathbf{v})\sum_{\mathbf{q}\in\mathbb{Z}^2}\hat{c}(\mathbf{q})e^{\frac{i\pi(\mathbf{q}\cdot\mathbf{v})}{l}}\,\mathrm{d}\,\mathbf{v} = \frac{1}{4l^2}\iint\limits_{\Omega} J(\mathbf{x}-\mathbf{v})\lim_{|R|\to\infty}\sum_{\mathbf{q}\in R}\hat{c}(\mathbf{q})e^{\frac{i\pi(\mathbf{q}\cdot\mathbf{v})}{l}}\,\mathrm{d}\,\mathbf{v} =$$
$$\frac{1}{4l^2}\iint\limits_{\Omega}\lim_{|R|\to\infty}\left(\sum_{\mathbf{q}\in R}\hat{c}(\mathbf{q})J(\mathbf{x}-\mathbf{v})e^{\frac{i\pi(\mathbf{q}\cdot\mathbf{v})}{l}}\right)\mathrm{d}\,\mathbf{v} = \frac{1}{4l^2}\iint\limits_{\Omega}\lim_{|R|\to\infty} f_R(\mathbf{v})\,\mathrm{d}\,\mathbf{v}.$$

I have $\lim_{|R|\to\infty} f_R(\mathbf{v}) = J(\mathbf{x}-\mathbf{v})n(\mathbf{v})$ for any $\mathbf{v} \in \mathbb{R}^2$, and based on conditions (B.6) there exists a function g such that $|f_R(\mathbf{v}| \leq g(\mathbf{v})$ for any vector R and $\mathbf{v} \in \mathbb{R}^2$ with $\iint_\Omega g(\mathbf{v})\,\mathrm{d}\,\mathbf{v} < \infty$. Therefore I could apply Lebesgue's dominated convergence theorem [1] once more and I have obtained

$$J * n(\mathbf{x}) = \lim_{|R|\to\infty}\left(\frac{1}{4l^2}\sum_{\mathbf{q}\in R}\hat{c}(\mathbf{q})e^{\frac{i\pi(\mathbf{q}\cdot\mathbf{x})}{l}}\iint\limits_{\Omega} J(\mathbf{x}-\mathbf{v})e^{\frac{i\pi(\mathbf{q}\cdot(\mathbf{v}-\mathbf{x}))}{l}}\,\mathrm{d}\,\mathbf{v}\right) = \frac{1}{4l^2}\sum_{\mathbf{q}\in\mathbb{Z}^2}\hat{J}\left(\frac{\pi\mathbf{q}}{l}\right)\hat{c}(\mathbf{q})e^{\frac{i\pi(\mathbf{q}\cdot\mathbf{x})}{l}}.$$

In a similar manner I have obtained

$$J * \bar{m}(\mathbf{x}) = \frac{1}{4l^2}\sum_{r\in\mathbb{Z}^2}\hat{J}\left(\frac{\pi\mathbf{r}}{l}\right)\bar{\hat{d}}(\mathbf{r})e^{\frac{-i\pi(\mathbf{r}\cdot\mathbf{x})}{l}}.$$

This implies

$$< J * n, m >= \iint\limits_{\Omega}(J * n(\mathbf{x}))\bar{m}(\mathbf{x})\,\mathrm{d}\,\mathbf{x} =$$
$$\frac{1}{16l^4}\sum_{\mathbf{r}\in\mathbb{Z}^2}\sum_{\mathbf{q}\in\mathbb{Z}^2}\hat{c}(\mathbf{q})\hat{J}\left(\frac{\pi\mathbf{q}}{l}\right)\bar{\hat{d}}(\mathbf{r})\iint\limits_{\Omega} e^{\frac{i\pi(\mathbf{q}\cdot\mathbf{x})}{l}} e^{\frac{-i\pi(\mathbf{r}\cdot\mathbf{x})}{l}}\,\mathrm{d}\,\mathbf{x} = \frac{1}{4l^2}\sum_{r\in\mathbb{Z}^2}\hat{c}(\mathbf{r})\bar{\hat{d}}(\mathbf{r})\hat{J}\left(\frac{\pi\mathbf{r}}{l}\right)$$

and

$$< n, J * m >= \iint\limits_{\Omega} n(\mathbf{x})(J * \bar{m}(\mathbf{x}))\,\mathrm{d}\,\mathbf{x} =$$
$$\frac{1}{16l^4}\sum_{\mathbf{q}\in\mathbb{Z}^2}\sum_{\mathbf{r}\in\mathbb{Z}^2}\hat{c}(\mathbf{q})\bar{\hat{d}}(\mathbf{r})\hat{J}\left(\frac{\pi\mathbf{r}}{l}\right)\iint\limits_{\Omega} e^{\frac{i\pi(\mathbf{q}\cdot\mathbf{x})}{l}} e^{\frac{-i\pi(\mathbf{r}\cdot\mathbf{x})}{l}}\,\mathrm{d}\,\mathbf{x} = \frac{1}{4l^2}\sum_{q\in\mathbb{Z}^2}\hat{c}(\mathbf{q})\bar{\hat{d}}(\mathbf{q})\hat{J}\left(\frac{\pi\mathbf{q}}{l}\right)$$

and concludes the proof of $< n, J * m > = < J * n, m >$ in the case of a finite neuronal network. It implies that equation (B.5) holds and in turn implies that the linear operator L_0^* is indeed the adjoint operator of the linear operator L_0 for finite neuronal networks.

Appendix C

The Matlab-code used for numerical simulations with the model

```
function CorticalSheet
%
% CorticalSheet
%
% Development of the firing rate of the neurons in the cortical sheet over
% 'Iterations' time steps. In this cortical sheet, consisting of
% integrate-and-fire neurons on a square grid, different types of travelling
% and oscillating wave pattern can be obtained. The type of pattern that
% stabilizes, is dependent on the values chosen for the parameters of the
% model.
%
% In this file, the following is done. First some constants are specified
% and a movie file is created. Next the fully symmetric (sparse) synaptic
% coupling matrix is constructed. Then the initial conditions are set after
% which the development is executed. A movie of the development is
% constructed. The numerical integration of the differential equations
% describing the model, the firing rate function and the Mexican hat function
% are given at the end of the file.
%
% CorticalSheet code -- (c) Januari 2012 D.C. Koppenol

%% Constants

% Number of iterations over which the model of the cortical sheet develops:

Iterations = 5100;

% Number of iterations whereafter the movie is created:

StartMovie = 5000;

% Number of neurons along one side in the model:

N = 60;

%% Creation of the movie file

mov = avifile('CorticalSheetDevelopment.avi','Compression','None');
mov.FPS = 10; mov.COLORMAP = colormap(jet(256));
mov.VIDEONAME = 'Development of the Firing Rate';
```

```
%% Determination of the sparse recurrent synaptic coupling matrix

y = 0:(N/2)-1;
y((N/2)+1:N) = -(-N/2:-1);
yy = repmat(y,1,N);
YY = zeros(N,N^2);
YY(1,:) = yy;

for i = 2:N
    YY(i,i:N^2) = YY(1,1:N^2-i+1);
    YY(i,1:(i-1)) = YY(1,N^2-i+2:N^2);
end

x = YY(1,:);
x = reshape(x,N,N);
xx = zeros(1,N^2);

for i = 1:N:N^2
    xx(1,i:(i+N-1)) = x((i+N-1)/N,:);
end

XX = zeros(N,N^2);
XX(1,:) = xx;

for i = 2:N
    XX(i,N*(i-1)+1:N^2) = XX(1,1:N^2-(i-1)*N);
    XX(i,1:N*(i-1)) = XX(1,N^2-N*(i-1)+1:N^2);
end

% Threshold between which the strength of the synaptic coupling is set to
% zero:

thresh = 0.01;

ii = zeros(1,3000000);
jj = zeros(1,3000000);
s = zeros(1,3000000);
nz =  0;

for i = 1:N^2

    d = sqrt(((XX(1+floor((i-1)/N),:)).^2) + (YY(1+mod((i-1),N),:).^2));
    j = mexhat(d);
    sj = find(abs(j) > thresh);

    if nz + length(sj) > length(s)

        s = [s, zeros(1,500000)];
        ii = [ii, zeros(1,500000)];
        jj = [jj, zeros(1,500000)];

    end

    s((nz+1):(nz+length(sj))) =  j(sj);
    ii((nz+1):(nz+length(sj))) =  i*ones(1, length(sj));
    jj((nz+1):(nz+length(sj))) =  sj;
    nz = nz + length(sj);

end
```

```
ii = ii(1:nz);
jj = jj(1:nz);
s = s(1:nz);
J = sparse(ii,jj,s, N^2, N^2);
clear i x y yy xx ii jj s nz XX YY

%% Initialization of the start condition

Ui = rand(N^2,1); % Initial firing rate of the neurons
Ai = zeros(N^2,1); % Initial adaptation of the neurons

%% Execution of the development of the firing rate of the neurons in the
%% cortical sheet

for k = 1:Iterations

    if mod(k,1000) == 0
        disp(k)
    end

    [Uo,Ao] = rateN(Ui,Ai,J);
    Ui = Uo;
    Ai = Ao;

    if k > StartMovie

        figure(1); clf;
        set(figure(1),'position',[10 210 500 500])

        imagesc(reshape(Ui,N,N))
        colorbar
        axis equal tight
        title('Development of the Firing Rate')
        drawnow;
        M = getframe(figure(1));
        mov = addframe(mov,M);

    end
end

mov = close(mov);

%% Numerical integration of the differential equations for the firing rate
%% and adaptation of the individual neurons

% 'dt' determines the size of the time step, 'tau' is the time constant,
% 'g' is the gain of the adaptation, and alpha is the parameter that
% controls the strength of the synaptic coupling.

function [Uo,Ao] = rateN(Ui,Ai,J)

dt = 0.1;
g = 4;
alpha = 1;
tau = 5;

SumU = J*Ui;

Uo = dt*(-Ui + F(alpha*SumU - g*Ai)) + Ui;
Ao = dt*(-Ai + Ui)/tau + Ai;
```

```
%% The firing rate function

function Fo = F(Ui)

r = 3;
eta = 0.5;

Fo = ((1 + exp(r*eta))/r)*((1 - exp(-r*Ui))./(1 + exp(-r*(Ui - eta))));

%% The Mexican hat function

function j = mexhat(d)

% A mexican hat function for use in the construction of the synaptic
% coupling matrix of the cortical sheet.

A = 70;
B = 125;
a = 0.1;
b = 0.03;

j = (A*a*exp(-a*d.^2) - B*b*exp(-b*d.^2))/3.141592;
```

References

[1] R.G. Bartle. *The Elements of Integration and Lebesgue Measure*. Mathematics Special Topics. Wiley Online Library, 1995.

[2] P.C. Bressloff, J.D. Cowan, M. Golubitsky, and P.J. Thomas. Scalar and pseudoscalar bifurcations motivated by pattern formation on the visual cortex. *Nonlinearity*, 14:739–775, 2001.

[3] R.D. Chervin, P.A. Pierce, and B.W. Connors. Periodicity and directionality in the propagation of epileptiform discharges across neocortex. *Journal of Neurophysiology*, 60:1695–1713, 1988.

[4] B.W. Connors and M.J. Gutnick. Intrinsic firing patterns of diverse neocortical neurons. *Trends in Neuroscience*, 13:99–104, 1990.

[5] R. Curtu. *Waves and Oscillations in Model Neuronal Networks*. PhD thesis, University of Pittsburgh, 2003.

[6] R. Curtu and B. Ermentrout. Pattern formation in a network of excitatory and inhibitory cells with adaptation. *SIAM Journal of Applied Dynamical Systems*, 3(3):191–231, 2004.

[7] G.B. Ermentrout and D. Kleinfeld. Traveling electrical waves in cortex: Insights from phase dynamics and speculation on a computational role. *Neuron*, 29:33–44, 2001.

[8] L. Grafakos. *Classical Fourier analysis*. Graduate texts in mathematics. Springer, 2008.

[9] D. Hansel and H. Sompolinsky. Modeling feature selectivity in local cortical circuits. In *Methods in Neuronal Modeling: From Ions to Networks*. 2nd edition.

[10] S.Y. Huang and S.S. Cheng. Absence of positive roots of sextic polynomials. *Taiwanese Journal of Mathematics*, 15(6):2609–2646, 2011.

[11] D.C. Koppenol. Models of self-organizing development of an attractor layer for entorhinal grid cells. Master's thesis, Universiteit van Amsterdam, 2008.

[12] A.G. Ramm. A simple proof of the fredholm alternative and a characterization of the fredholm operators. *American Mathematical Monthly*, 108:855–860, 2001.